

Unifying the Efforts of Medicine, Chemistry, and Engineering in Biosensing Technologies to Tackle the Challenges of the COVID-19 Pandemic

Özgecan Erdem, Ismail Eş, Yeşeren Saylan, and Fatih Inci*



Cite This: <https://doi.org/10.1021/acs.analchem.1c04454>



Read Online

ACCESS |

Metrics & More

Article Recommendations

CONTENTS

A Short Snapshot on Earlier Infections and COVID-19

Molecular Aspects and Transmission of SARS-CoV-2
Current Platforms for COVID-19 Diagnosis
Recent Progress in COVID-19 Diagnostic Technologies

Sensor Systems

Electrochemical Sensing Modality

Optical Sensing Modality

Field-Effect Transistor Biosensors

Lateral Flow Assays

Clustered Regularly Interspaced Short Palindromic Repeats Strategy

Future Directions and Integration of Other Technologies

In Silico Models to Curb the Pandemic

Internet of Things: Expanding the Geography for Data Collection/Analysis during the COVID-19 Diagnosis Using Secure Cloud Settings

Artificial Intelligence Technologies and Strategies: Standardizing Test Results and Significantly Reducing the Workload in the Clinic

Wearable Platforms and Mobile Phone Systems: Adaptation of Platforms for Daily Use

Conclusion

Author Information

Corresponding Author

Authors

Notes

Biographies

Acknowledgments

References

A

B

B

F

F

G

H

K

L

O

p

P

Q

Q

Q

Q

R

S

S

S

S

S

S

S

S

World Health Organization (WHO), SARS emerged as an acute respiratory disease (2003) with the capability of rapid transmission, and it accounted for 8096 cases and 774 deaths worldwide between November 2002 and July 2003.⁵ Studies have been conducted to track down whether SARS-CoV is excreted permanently through respiratory secretions and/or enteric pathways of asymptomatic patients. Host-dependent factors such as age, genotype, immune status, stress, and secondary infection with other microorganisms (e.g., viruses, parasites, or bacteria) affect the susceptibility of diseases caused by CoV. It is urgent to find out which host factors and virus types are responsible for the superspreading events witnessed with SARS. In the SARS epidemic, most patients were infected by close and/or short-term contact with people, who were SARS-CoV positive.⁶ A decade after the SARS epidemic, people faced another emerging disease caused by a new beta-coronavirus (β -CoV), Middle East Respiratory Syndrome-Coronavirus (MERS-CoV), which is a zoonotic origin of Coronavirus. The first case of MERS-CoV was identified from an individual with pneumonia in Saudi Arabia.^{7–9} Despite earlier efforts on seeking the reservoir of MERS-CoV in bats, the serological analysis revealed a superior prevalence of MERS-CoV-neutralizing antibodies in dromedary camels living in Oman and the Canary Islands,¹⁰ which were further supported with two cases of MERS, who had close contact with these animals in Qatar.¹¹ MERS-CoV infection in humans is explained by infected dromedary camels in most regions, and it has been spread through zoonotic transmission. However, when looking at the spread of SARS-CoV, it does not appear to cause many infections in human populations with relatively rare human–bat interactions without an infected intermediate host.

In December 2019, a group of patients diagnosed with unknown pneumonia was hospitalized in Wuhan, Hubei Province, China. While investigating patient stories, a pivotal link between humans, seafood, and the wet animal wholesale

Special Issue: Fundamental and Applied Reviews in Analytical Chemistry 2022

A SHORT SNAPSHOT ON EARLIER INFECTIONS AND COVID-19

In the last decades, we have faced several infectious diseases, transiting their statuses from epidemics to pandemics that affect multiple regions across the globe. As an example, Severe Acute Respiratory Syndrome-Coronavirus (SARS-CoV) is the causative agent of SARS, which is transmitted through wild animals, i.e., Himalayan palm musks.^{1–4} As reported by the

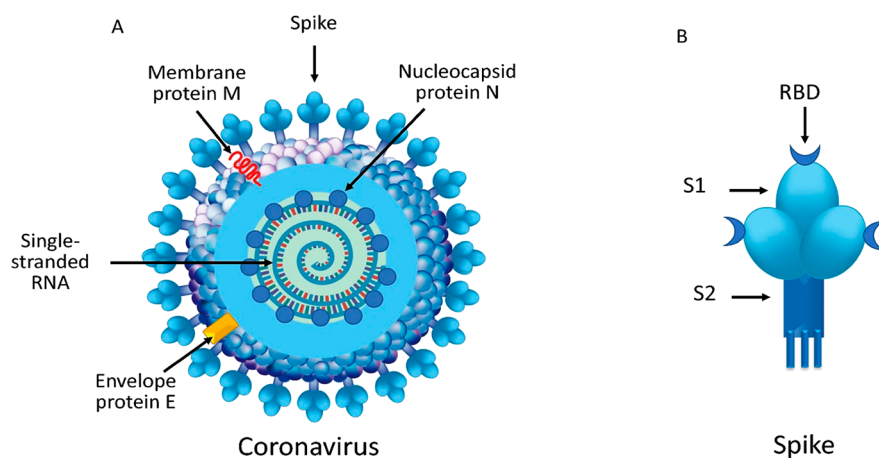


Figure 1. SARS-CoV-2 Virus. (A) SARS-CoV-2 virion and proteins. (B) Spike protein of SARS-CoV-2 [Reprinted with permission from Rossi, G. A.; Sacco, O.; Mancino, E.; Cristiani, L.; Midulla, F. Differences and Similarities between SARS-CoV and SARS-CoV-2: Spike Receptor-Binding Domain Recognition and Host Cell Infection with Support of Cellular Serine Proteases. *Infection* 2020, 48, 665–669 (ref 185). Copyright 2020 Springer].

market was observed, and further sequencing examinations on the samples collected from patients' airway epithelial cells revealed a previously unknown beta-coronavirus, first named 2019-nCoV, and then, called SARS-CoV-2.^{12,13} While the preliminary investigation is limited to the infection around a single animal market, the world has then experienced rapid transmission from person-to-person through the release of respiratory fluids during exhalation or direct contact.¹⁴ After the first incidents began, the Chinese government started to apply immediate country-wide restriction measures of unprecedented scope of extreme public health protection efforts launched to counteract the spread of the disease. These measures include a regional lockdown of more than 50 million people, severe travel restrictions, and mandatory quarantines to control the disease during a rush travel time through the Chinese New Year. Within a few weeks, COVID-19 cases were also reported in other countries.¹⁵

According to the WHO COVID-19 situation report, as of November 2021, there are ~250 million confirmed cases, ~5 million of which resulted in death in 221 countries and territories worldwide. Early detection and immediate isolation of diagnosed patients have been two critical measures for a successful response to the COVID-19 pandemic. In this regard, international regulatory organizations such as WHO have earnestly and persistently urged the scientific community to focus on the rapid manufacturing of reliable diagnostic devices to make prompt decisions to forestall the spread of the infection. In this manner, this review aims to outline recent biosensing technologies developed for rapid, early, and reliable diagnosis of COVID-19. Here, molecular aspects and transmission of SARS-CoV-2 will be briefly introduced, and then, current biosensing platforms will be comprehensively discussed, underscoring their pros and cons.

MOLECULAR ASPECTS AND TRANSMISSION OF SARS-COV-2

Similar to the other coronaviruses, the SARS-CoV-2 genome comprises a single-stranded RNA with 30 kb nucleotides encoding four main structural proteins: (1) spike (S), (2) envelope (E), (3) membrane (M), and (4) nucleocapsid (N) protein (Figure 1A–B).¹⁶ S proteins particularly assist viral interactions with the entry into host cells through target

receptor proteins, i.e., angiotensin-converting enzyme 2 (ACE2).^{17–19} ACE2 has been primarily determined as an enzyme catalyzing the conversion of angiotensins, and it is expressed in vascular endothelial cells in heart and kidney, as well as small intestine, testis, thyroid, and adipose tissue, and subsequently recognized as the receptor to which SARS-CoV binds to invade our cells.^{16,20} Over the course of viral interactions with the host, ACE2 connects to the receptor-binding motif in the receptor-binding domain of SARS-CoV-2, thus acting as the receptor for SARS-CoV-2.¹⁶ Once this binding occurs, a nearby host protease cleaves S proteins that release the fusion peptide, thereby enabling viral entry to the cells.²¹ E protein, on the other hand, is a small protein (71 amino acids long) with a short hydrophilic N-terminal, followed by a large hydrophobic region and a large hydrophilic C-terminal tail.²² This protein facilitates the release of the virus, hence playing a key role in COVID-19 pathogenesis.²³ Furthermore, M protein is the most abundant protein with a size ranging from 25 to 30 kDa, consisting of three transmembrane domains that start with a short NH₂-terminal domain and ending with a long COOH terminus.²⁴ N proteins are composed of three domains: (i) an N-terminal, (ii) a central Serine/Arginine-rich flexible linker domain, and (iii) a C-terminal domain. These proteins are critical for viral genome packaging, and they interfere with the defense system of host cellular, promoting apoptosis.^{25,26} Comprehensive understanding of the molecular aspects of these proteins is crucial as their interactions would be utilized to produce drug and vaccine candidates, as well as designing surface chemistry and recognition elements on biosensors.

CURRENT PLATFORMS FOR COVID-19 DIAGNOSIS

As experienced in past viral outbreaks, the success of diagnostic and screening strategies relies on practical and adequate sampling. Swab sampling, i.e., the first step of testing, is taken from the upper respiratory tract (particularly in the nasopharynx), where viruses are accommodated in a vast majority of cases. Proper collection of samples is the most critical step in the diagnosis process since any issues here may mislead outcomes, mostly false-negative/false-positive results that significantly delay clinical management, including treat-

Table 1. Comparison of Serological and Molecular Assays for Detection of SARS-CoV-2

properties	serological (lateral flow immunoassay)	molecular (RT-PCR)
target	IgM, IgG, total antibody	E gene, S gene, N gene, RdRP gene, ORF1ab region, ORF 8 region
sample preparation	blood/serum sample	nasopharyngeal or oropharyngeal swabs
assay time	10–15 min	4–6 h including sample collection and sample pre-processing
analysis	lateral flow immunoassay	Real-time Reverse Transcriptase (RT)-PCR
labor-intensive	no requirement for additional equipment	reagent and equipment requirements, technically complex procedure
cost	low cost	costly assay
false \pm results	false-negative results (if the test is conducted too early and antibodies have not developed yet)	false-negative result (if the level of viral RNA in the sample is too low for the detection)

Table 2. Selected Commercial Lateral Flow Assay Platforms for Diagnosing COVID-19^a

company	assay type	target	regulatory status
AIVD Biotech Inc.	SARS-CoV-2 antigen detection rapid lateral flow test	antigen	RUO
Avacta Life Sciences Ltd.	AffIDx SARS-CoV-2 lateral flow antigen test	antigen	in development
Beijing Tigsun Diagnostics Co., Ltd.	Tigsun COVID-19 combo IgM/IgG rapid test (lateral flow method)	antibody	India CDSCO, CE-IVD
Elabscience	SARS-CoV-2 (2019-nCoV) IgG/IgM lateral flow assay kit (whole blood/serum/plasma)	antibody	RUO
Genobio Pharmaceutical Co., Ltd.	COVID-19 IgG/IgM lateral flow assay	antibody	CE-IVD
	COVID-19 IgG lateral flow assay	antibody	CE-IVD
	COVID-19 IgM lateral flow assay	antibody	CE-IVD
	COVID-19 antigen lateral flow assay	antigen	CE-IVD
Guangzhou Wondfo Biotech Co., Ltd.	Wondfo SARS-CoV-2 antibody test (lateral flow method)	antibody	Singapore HSA, China NMPA EUA, Australia TGA, Brazil ANVISA, India CDSCO, CE-IVD
JOYSBIO (Tianjin) Biotechnology Co., Ltd.	COVID-19 neutralizing antibody test kit (lateral flow test)	antibody	CE-IVD
Koch Biotechnology (Beijing) Co., Ltd.	SARS-CoV-2 antigen lateral flow assay	antigen	UK MHRA
Quick Energy Technologies Limited	MediKit COVID-19 antibody test (IgM/IgG lateral flow assay)	antibody	CE-IVD
Shanghai LiangRun Biomedicine Technology Co. Ltd.	diagnostic kit for IgM/IgG antibody of SARS-CoV-2 (colloidal gold/lateral flow assay)	antibody	Brazil ANVISA, Singapore HSA, CE-IVD
Tianjin Era Biology Technology Co., Ltd.	COVID-19 IgM/IgG lateral flow assay	antibody	CE-IVD
	COVID-19 IgM lateral flow assay	antibody	CE-IVD
	COVID-19 IgG lateral flow assay	antibody	CE-IVD
Dynamiker	lateral flow test cassette	antibody	CE-IVD
Sure Bio-Tech (USA) Co., Ltd.	lateral flow test cassette	antibody	CE-IVD
CTK Biotech, Inc.	lateral flow immunoassay	antibody	Australia TGA, Brazil ANVISA, India CDSCO
Atlas Medical	lateral flow immunochromatographic assay	antibody	CE-IVD
Acon Biotech (Hangzhou) Co., Ltd.	lateral flow test cassette	antibody	CE-IVD

^aThis list shows some selected examples of assays stated on the source FINDdx.¹⁸³ **Abbreviations:** RUO (Research Use Only); FDA EUA (Food and Drug Administration Emergency Use Authorization); CE-IVD (Conformité Européenne-in vitro diagnostics); ANVISA (The Brazilian Health Regulatory Agency); WHO EUL (World Health Organization Emergency Use Listing Procedure); TGA (Therapeutic Goods Administration); CDSCO (Central Drugs Standard Control Organization); NMPA EUA (National Medical Products Administration Emergency Use Authorization); UK MHRA (United Kingdom's Medicines and Healthcare products Regulatory Agency).

ment and control of the disease. Due to any possible fluctuations in the results, the Centers for Disease Control and Prevention (CDC) has released a guideline to standardize the procedure of specimen collection.²⁷ Once samples are correctly taken, either qualitative and/or quantitative tests are employed to confirm and define the stage of infection. In this manner, existing diagnostic tools rely on molecular trace of the viral agent^{28,29} and serological markers.³⁰ In addition to the samples from the upper respiratory tract, increasing evidence indicates that the gut may be another location, where the virus is located and samples from the gut would greatly impact the identification of an asymptomatic person that could possibly spread the infection. Interestingly, even if the nasopharyngeal test result is negative, viral RNA could be found in rectal swabs

of an asymptomatic person.³¹ Therefore, sampling with either nasopharyngeal, oropharyngeal, or rectal swabs is critical to proceed with a diagnostic test.

Immunoassays and nucleic acid-based diagnostic assays have been largely implemented during the pandemic (Table 1).³² Briefly, immunoassays are designed to determine viral antigens or antibodies (IgM and IgG) against SARS-CoV-2 (serological assays). Especially, due to their facile sampling and rapid process, serological assays are executed on lateral flow assays (LFA), focusing on detecting serum antibodies against viral structural proteins. A number of clinical diagnostic kits have been manufactured and tested using serum samples. Here, we provide an up-to-date list of the selected commercial lateral flow assay platforms, focusing on the detection of SARS-CoV-2

Table 3. Selected Commercial Biosensing Platforms Approved by USA FDA EUA for the Detection of SARS-CoV-2^a

company	assay type	target
Access Bio, Inc.	CareStart COVID-19 IgM/IgG	antibody
ACON Laboratories, Inc.	ACON COVID-19 IgG/IgM rapid test	
Assure Tech. (Hangzhou) Co., Ltd.	COVID-19 IgG/IgM rapid test device	
Autobio Diagnostics Co., Ltd.	anti-SARS-CoV-2	
Beijing Wantai Biological Pharmacy Enterprise Co., Ltd.	Wantai SARS-CoV-2 Ab rapid test	
Biocan Diagnostics Inc.	Tell Me Fast novel coronavirus (COVID-19) IgG/IgM Ab test	
BIOHIT HealthCare (Hefei) Co., Ltd.	SARS-CoV-2 IgM/IgG antibody test kit (colloidal gold method)	
Cellex Inc.	Cellex qSARS-CoV-2 IgG/IgM cassette rapid test	
Hangzhou Biotest Biotech Co., Ltd.	RightSign COVID-19 IgG/IgM rapid test cassette	
Hangzhou Laihe Biotech Co., Ltd.	LYHER novel coronavirus (2019-nCoV) IgM/IgG antibody combo test kit (colloidal gold)	
Jiangsu Superbio Biomedical Technology (Nanjing) Co., Ltd.	SARS-CoV-2 (COVID-19) IgM/IgG antibody fast detection kit (colloidal gold)	
Medigen Biotechnology Corp.	TBG SARS-CoV-2 IgG/IgM rapid test kit	
Megna Health	Megna Health rapid COVID-19 antibody (IgM/IgG) combo test kit	
NanoEntek Inc.	FREND COVID-19 total Ab	
ScheBo Biotech AG	ScheBo SARS-CoV-2 quick IgM/IgG	
Snibe Co., Ltd. (Shenzhen New Industries Biomedical Engineering Co., Ltd.)	MAGLUMI 2019-nCoV IgG (CLIA)	
Xiamen Biotime Biotechnology Co., Ltd.	SARS-CoV-2 IgG/IgM rapid, qualitative test kit	
Cellex Inc.	BinaxNOW COVID-19 Ag card	antigen
Abbott Laboratories	NAVICA mobile app and BINAXNOW COVID-19 Ag card	
Access Bio Inc.	CareStart COVID-19 antigen	
Becton Dickinson & Company	BD Veritor system for rapid detection of SARS-CoV-2	
LumiraDx UK Ltd.	LumiraDx SARS-CoV-2 Ag test	
Quidel	Sofia 2 Flu + SARS antigen FIA	
Quidel	Sofia 2 SARS antigen FIA	
Spring Healthcare Services AG	SARS-CoV-2 antigen rapid test cassette (swab)	

^aThis list was prepared using the source FINDdx.¹⁸³

(Table 2). For instance, in a clinical study of 1020 serum samples, a SARS-CoV-2 IgG assay from Abbott, which was approved by FDA, resulted in 99.9% specificity.³³ Another study reported antibody response against SARS-CoV-2 in 285 infected patients and revealed IgG positive in all patients within 19 days right after the beginning of symptoms.³⁴ Production of antibodies from the entry of the virus into the body occurred simultaneously or in sequence and then became detectable in blood circulation. Both IgG and IgM titers reached a plateau within 6 days following the seroconversion. In addition, these tests were able to monitor immunological status during postrecovery,^{32,35} and they would guide us on the epidemiology of the disease and the immune status of asymptomatic patients. However, serological assays are not immediate measurements of viral presence and infection since serological markers exist for 4–10 days for IgM and ~2 weeks for IgG.³⁶ The sensitivity of LFAs is another limiting factor due to the level of antibody production needs to achieve the limit of detection (LOD) of the assay. In addition to all these challenges, cross-reactivity of immunoglobulins produced in earlier SARS-CoV could impede the diagnosis of COVID-19 for effective clinical management.

In the current practice, molecular techniques, e.g., reverse transcription (RT) polymerase chain reaction (PCR)³⁷ or real-time RT-PCR,³⁸ are the other most utilized strategies. As reported in patients with SARS-CoV-2 infection, for instance, huge viral loads have been encountered in the upper and lower respiratory tract 5–6 days after the beginning of symptoms.³² RT-PCR tests may have yielded early negative results in the upper respiratory tract as the infection originates first in the alveolar cells. Most studies, however, have showed that samples

from the nasopharyngeal area are more appropriate to use from the onset of symptoms in detecting SARS-CoV-2 than that from the oropharyngeal area.^{35,39–42} Although viral RNA could also be detected 2 weeks after the onset of the disease, the viral load would drop in the course of this time frame. Samples taken at different stages, moreover, may yield fluctuations in the results, such as positive/negative outcomes or alterations in viral load levels.³⁹

Consequently, more than one parameter should be examined for such molecular tests to better understand the infection status and stages. Despite the utility and expansion of molecular tests to the clinic and research laboratories, they are complex, costly, and lengthy (4–6 h) with labor-intensive methods with multistep procedures such as lysis, RNA isolation, and amplification. Notably, all these procedures require trained personnel and specialized laboratories with appropriate biosafety levels. Still, from a biological perspective, the sensitivity and reliability of these methods are questioned because of negative results in some patients suspected of having the disease and positive results in some cases with confirmed recovery. As well, the limitations in their sensitivity and any errors in sample collection might miss low viral load levels. Considering these drawbacks, the current situation hence urges the development of rapid testing for diagnosing individuals.^{43,44}

Overall, as of October 2021, the FIND (Foundation for Innovative New Diagnostics) organization has listed 1127 commercialized molecular and serological assays available on the market. A list of biosensing platforms used as rapid diagnostic assays approved by the Food and Drug Admin-

Table 4. Recent Technologies for the Detection of SARS-CoV-2^a

test type	sample source	target	assay time	limit of detection	refs
Electrochemical Systems					
electrochemical immunoassay	nasopharyngeal swab	S and nucleocapsid protein	30 m	19 and 8 ng/mL	56
electrochemical immunosensor	saliva and oropharyngeal swab	S protein	35 m	0.01 ag/mL	57
potentiostat-based sensor	saliva	S protein	10–30 s	90 fM	58
electrochemical biosensor	nasal swab	S protein	NR	276 fmol/L	59
electrochemical biosensor	NR	RdRp and nucleocapsid gene	<20 m	0.972 and 3.925 fg/uL (10^3 – 10^9 copies/mL)	60
organic electrochemical transistor	serum	IgG	5 m	10 fM	61
organic electrochemical transistor	nasopharyngeal swab and saliva	S protein	10 m	23 fM (2700 to 1.8×10^{12} copies/mL)	62
electrochemical dual-aptamer biosensor	serum	nucleocapsid protein	NR	8.33 pg/mL	69
electrochemical aptamer biosensor	serum and artificial saliva	S protein	15 s	picomolar levels (1 to 100 copies/mL)	70
screen-printed carbon electrode platform	spiked in PBS buffer	S protein	40 m	1.30 pM	71
FET-Based Biosensors					
FET-based sensor	nasopharyngeal swab	S protein	2 m	2.42×10^2 copies/mL	105
graphene field-effect transistor sensor	spiked in PBS buffer	S1 protein	2 m	0.2 pM	106
silicon-based FET biosensor	nasal swab	SARS-CoV-2	NR	0.002 fM	107
FET nanosensor	throat swab	SARS-CoV-2 RNA	2 m	2.29 fM	108
tungsten diselenide-based FET system	spiked PBS buffer	S protein	80 s	25 fg/ μ L	109
SWCNT-based FET	nasopharyngeal samples	S and nucleocapsid protein	2 m	0.55 and 0.016 fg/mL	111
Optical Systems					
surface plasmon resonance sensor	serum	nucleocapsid antibodies	15 m	1 μ g/mL	83
localized surface plasmon resonance sensor	simulated multisequence mixture	RdRp and ORF1ab genes	NR	0.22 pM (1.13×10^8 copies/mL)	1
interferometric optical	saliva and serum	IgG, IgM, and IgA	3 h	NR	84
plasmonic sensor	spiked buffer	SARS-CoV-2 pseudoviruses	15 m	370 vp/mL	85
fiber-optic platform	serum	S protein	NR	1 and 10^8 pg/mL	86
SPR aptasensor	serum	nucleocapsid gene	1000 s	4.9 pg/mL	87
optical microfiber aptasensor	serum	nucleocapsid protein	3 m	6.25×10^{-19} M	88
microfluidic-integrated optical biosensor	serum	IgM and IgG	<7 m	0.82 and 0.45 ng/mL	100
photonic crystal biosensor	serum	S protein	15 m	100 pg/mL	101
Lateral Flow Immunoassays					
AuNP-based assay	serum	nucleocapsid proteins	15–20 m	NR	114
AuNP-based assay	RNA standards	2 RdRp and nucleocapsid genes	80 m	20 copies	115
dual lateral flow optical/chemiluminescence immunosensors	saliva	IgG and IgM	15 m	NR	116
optical-based assay	blood	IgM and IgG	<10 m	0.362 ng/mL	118
microfluidic-integrated assay	throat-nasopharyngeal swabs	RNA	30 m	1 copy/mL	119
lanthanide-doped nanoparticle-based assay	serum	IgG	10 m	NR	126
quantum dot nanobead-based assay	serum	IgG and IgM	<15 m		127, 128
multiplex RT-LAMP combined	swab	ORF1ab and nucleoprotein genes	1 h	12 copies	131
aggregation-induced near-infrared emission nanoparticle-labeled assay	serum	IgM and IgG	1–7 days	0.236 and 0.125 μ g/mL	132
nanoparticle fluorescence immunoassay	plasma	IgG, IgM, and IgA	3–10 m	NR	133
SERS-based platform	serum	IgM and IgG	25 min	1 pg/mL	134
CRISPR Strategy					
CRISPR-based DNA detection	NR	RdRp gene	10–30 m	1×10^4 copies/mL	143
CRISPR-based nucleic acid detection	NR	NR	1–3 h	10 copies/ μ L	142
CRISPR-based paper strip assay	saliva	ORF1b gene	2–3 h	10 copies/ μ L	137
CRISPR-Cas 12 based lateral flow assay (DETECTR)	respiratory swabs	E and N genes	30–40 m	10 copies/ μ L	144
CRISPR-mediated assay	saliva and nasopharyngeal swabs	N gene	60 m	100 viral genomes	145
CRISPR nucleic acid detection platform	oropharynx swab samples	ORF1ab and nucleoprotein	60 m	10 copies	146

Table 4. continued

test type	sample source	target	assay time	limit of detection	refs
CRISPR/Cas12a-enhanced colorimetry assay	cultured virus	RNA	NR	50 copies	184
CRISPR/Cas12/CrRNA LFA assay	patient samples	ORF1ab and nucleoprotein	60 m	7 copies	147

^aNR: Not reported.

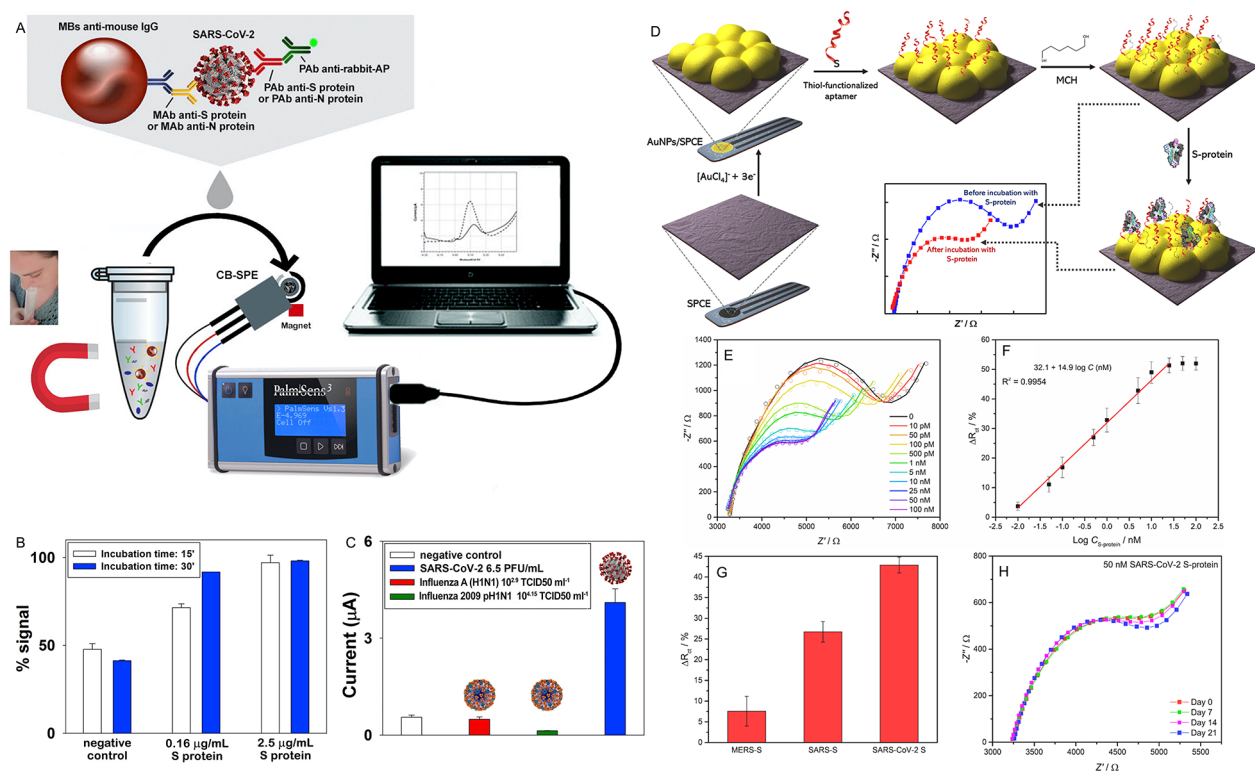


Figure 2. Electrochemical detection of SARS-CoV-2 virus. (A) Magnetic bead-based assay for the detection of SARS-CoV-2 in untreated saliva. (B) Effect of incubation time (15 and 30 min) on the signal response of the biosensor. (C) A comparative study between SARS-CoV-2 (6.5 PFU/mL), seasonal influenza virus A (H1N1) ($10^{2.9}$ TCID₅₀ mL⁻¹), and influenza 2009 pH1N1 virus ($10^{4.15}$ TCID₅₀ mL⁻¹) [Reprinted with permission from Fabiani, L.; Saroglia, M.; Galatà, G.; De Santis, R.; Fillo, S.; Luca, V.; Faggioni, G.; D'Amore, N.; Regalbuto, E.; Salvatori, P.; Terova, G.; Moscone, D.; Lista, F.; Arduini, F. Magnetic Beads Combined with Carbon Black-Based Screen-Printed Electrodes for COVID-19: A Reliable and Miniaturized Electrochemical Immunosensor for SARS-CoV-2 Detection in Saliva. *Biosens. Bioelectron.* **2021**, *171*, 112686 (ref 56). Copyright 2021 Elsevier]. (D) A stepwise manufacturing of aptasensor for detecting S protein of SARS-CoV-2. (E) Nyquist plots of the aptasensor response toward different concentrations of S-protein in PBS solution. (F) Calibration curve of the aptasensor with logarithmic S-protein concentration. (G) Selectivity of the aptasensor analyzed with the S-proteins of MERS-CoV, SARS-CoV, and SARS-CoV-2. (H) Impedimetric response obtained with 50 nM of SARS-CoV-2 S-protein to evaluate the stability of the aptasensor [Reprinted with permission from Abrego-Martinez, J. C.; Jafari, M.; Chergui, S.; Pavel, C.; Che, D.; Sij, M. Aptamer-Based Electrochemical Biosensor for Rapid Detection of SARS-CoV-2: Nanoscale Electrode-Aptamer-SARS-CoV-2 Imaging by Photo-Induced Force Microscopy. *Biosens. Bioelectron.* **2022** *195*, 113595 (ref 71). Copyright 2022 Elsevier].

istration for emergency use authorization (USA FDA EUA) is provided in Table 3.

RECENT PROGRESS IN COVID-19 DIAGNOSTIC TECHNOLOGIES

Early diagnosis is the mainstay to initiate the most efficient therapy, greatly accelerating life-saving decisions on treatment, as well as contributing to the control and potential prevention of an emerging pandemic. Hence, WHO has been urging all communities to perform massive diagnostic testing to curb virus transmission since testing aids researchers in learning the disease epidemiology. Despite centralized, well-equipped diagnostic facilities in developed countries, accessing diagnostic testing in the settings with scarce resources is still a huge concern due to economic and technological shortfalls in the healthcare system.⁴⁵ Considering the WHO's ASSURED (affordable, sensitive, specific, user-friendly, rapid and robust,

equipment-free, and deliverable to end-users) criteria,⁴⁶ newly developed/proposed technologies need to be evaluated studiously before their implementation to practice, and therefore, we construct this section to comprehensively assess diagnostic technologies and the associated strategies for restraining viral outbreaks, especially for the COVID-19 pandemic. All the studies demonstrated below are criticized through multiple parameters, such as a LOD, assay time, sample source, and target analytes (Table 4).

Sensor Systems. Healthcare systems have been in the midst of a paradigm transition from the centralized care to the point-of-care (POC) and the point-of-need (PON) settings.⁴⁷ In the course of this revolution, sensor systems have played one of the crucial roles by not only providing powerful alternatives to current analytical tools, but also paving the way to make them in portable and easy-to-use fashions.^{48,49} In particular, many sensors are well-aligned with functional and

precise nanostructures to address real-world problems in biomedicine.⁵⁰ As a classical definition, sensor systems are a kind of translator that first analyzes biological signals or interactions with target and recognition elements and, then, transfers (bio)chemical signals into an analytical entity, including electrical,⁵¹ mechanical,⁵² or optical signals.⁵³ Their applications are not limited to laboratory research and have been deployed into multiple settings, such as airports, borders, and public health offices, particularly for detecting infectious pathogens to manage outbreaks in a timely manner. Before applying such efforts from scratch, researchers have taken lessons from earlier outbreaks (e.g., SARS- and MERS-CoV) that could help fight current pandemics. In addition to their direct applications in SARS-CoV-2 detection, we here denote a variety of research focusing on diagnosing COVID-19. We believe that the biosensing platforms discussed here hold the potential to be adapted to the management of future viral outbreaks, thereby drawing new directions for the convenience of researchers in the field. One should keep in mind that each biosensing platform cited in the following section reports different kinds of LOD values, such as concentration of viral proteins/nucleic acids since their detection strategy and samples are distinct. Moreover, it was recently reported that each infected person approximately carries 10^9 – 10^{11} virions during peak infection, which corresponds to a total mass in the range of 1–100 μg of viral mass (a single viral particle has a mass of ~ 0.001 pg).⁵⁴ Given this information, the LOD values for each study can be roughly estimated, and the sensitivity of each biosensing platform can be assessed effectively.

Electrochemical Sensing Modality. Developing diagnostic tools with drastically low LOD and ultrafast analysis time is crucial to detect the early onset of COVID-19 infection. In such an emergency, electrochemical biosensors, composed of specific electrodes to translate chemical signals into an electrical signal, have been urgently employed as a promising diagnostic tool for COVID-19.⁵⁵ In particular, modifying electrodes is a major requisite to capture the structural proteins from SARS-CoV-2 with the lowest LOD possible. As an example from the recent literature, an electrochemical immunoassay biosensor was developed to detect SARS-CoV-2 S and N proteins in saliva obtained from nasopharyngeal swab specimens, which were then validated with PCR tests.⁵⁶ Here, the screen-printed electrodes were modified with carbon black nanomaterial, and the detection was performed through magnetic beads as the support of immunological chain reaction and secondary antibody for a labeling step (Figure 2A). Carbon black nanomaterials improved the sensitivity, and at the same time, magnetic beads increased the surface area to bind a high amount of capture antibody. Within 30 min, the assembled sensor provided 19 and 8 ng/mL of LOD values in serum for S and N protein, respectively (Figure 2B–C). Another biosensor was constructed through a glassy carbon electrode modified with gold-clusters, cysteamine, and glutaraldehyde in order to detect SARS-CoV-2 S proteins in saliva and oropharyngeal swab samples, and it was achieved to detect down to 0.01 ag/mL.⁵⁷ Recently, an in-house built sensor system (eCovSens) has been benchmarked with a commercial potentiostat system by detecting SARS-CoV-2 S protein in saliva.⁵⁸ In this study, the commercial potentiostat sensor was built on a fluorine-doped electrode, which was dropped onto the gold nanoparticle (AuNP), and its surface was then decorated with monoclonal anti-nCOVID-19 antibodies (Abs) to capture the target analytes. The measurement

strategy was designed to monitor the changes in electrical conductivity. The addition of antigens to the electrode alters the existing electrical current and the interactions between antigens and antibodies provides a highly specific response. With a similar measurement strategy, yet different structural electrode type, eCovSens was developed on screen-printed carbon electrodes, which were modified with anti-SARS-CoV-2 antibodies. In terms of detection range, both sensors were able to detect changes in electrical conductivity while monitoring antigen–antibody interactions within a wide concentration range (1 fM to 1 μM), and their lowest detectable levels in the spiked saliva samples were 90 and 120 fM for eCovSens and potentiostat, respectively. Due to its portability feature, the eCovSens system would be an exciting candidate for detecting SARS-CoV-2 antigens from patient saliva samples in a rapid manner.

Besides electrode modifications, coating an electrode surface with specific patterns composed of metal material enabled to enhance the detection efficiency. A highly uniform gold microcuboid pattern, for instance, was architected over an electrode surface to be employed as a microelectrode for detecting SARS-CoV-2 S proteins. It was able to measure these proteins as low as 276 fmol/L in positive samples, which were collected from nasal swabs.⁵⁹ Despite providing low detection limits, uniform distribution, size, and morphology of the patterns were key factors to meet reproducibility criteria of these sensors. Moreover, fine-tuning pattern topographies, for instance changing the pattern geometry, would be assessed to further improve the current LOD levels, because such a system is particularly advantageous for tracking the early onset of the disease much easier and more rapidly. As another example, a multielectrode biosensing platform was fabricated using multiple gold electrodes immobilized with various capture probes to test different SARS-CoV-2 proteins simultaneously.⁶⁰ Such a sensitive electrochemical biosensor in a patch format was further combined with recombinase polymerase amplification (RPA) driven by human body temperature. Briefly, the thiol-modified primers were immobilized on the working electrodes, and differential pulse voltammetry then determined the reduction of current density led by the hybridization reaction between RPA amplicon and primers as the amplicons accumulated on the electrode. A multimicroelectrode array detected both N and RdRP genes with the LOD values of 3.925 and 0.972 fg/ μL , respectively. Despite the self-driven feature of the assay based on body temperature, any changes or alterations on the temperature would potentially impact on the assay performance.

Organic electrochemical transistors have been previously reported as high-performance transducers for high-throughput detection of biomarkers, and for instance, they have been recently utilized for IgG detection of SARS-CoV-2.⁶¹ This sensing platform was developed through covalent immobilization of SARS-CoV-2 S proteins on the electrode, followed by detecting SARS-CoV-2 IgG through the S proteins. This system provided an affordable, label-free, and portable manners, detecting as low as 1 fM in an aqueous solution and 10 fM in serum and saliva within <5 min. The basic mechanism behind such a sensing system is the fact that positively charged IgG molecules generate electrical dipoles on the gate surfaces and adjust the current of the electrochemical sensor. Hence, electrolyte ion concentrations and pH values need to be optimized to achieve a desired device sensitivity. These values would significantly vary depending on the type of

viral proteins to be screened, hence the biosensor platform needs to be designed accordingly. Another organic electrochemical transistor was manufactured from a single molecule detection strategy, focusing on viral spike proteins in clinical nasopharyngeal swab and saliva samples.⁶² Briefly, the transistor was functionalized with a programmable receptor unit, containing a well-characterized anti-GFP nanobody linked to a SpyCatcher—a domain recognized by a short SpyTag peptide—on a gold electrode. The biosensing platform enabled results after 10 min of exposure and application of 5 μ L of samples, and it provided a LOD of 23 fM. Although the functionalization and fabrication steps of the sensor are simple, the current laboratory-scale prototype requires meticulous handling by a skilled person, which may potentially increase the interpersonal errors during the sample preparation and analysis. To overcome this issue, the device should be engineered into a single-housing flow-cell format for facile use by minimally trained persons for the expansion of its use.

On the other hand, one of the major impediments encountered in electrochemical biosensors to detect viral nucleic acid is the process of biofouling, which is the accumulation of biomolecules on a sensing surface. As a solution, an antifouling biosensor was basically designed using electropolymerized polyaniline nanowires and specific peptides to precisely detect the N phosphoprotein of the virus.⁶³ To construct the biosensor, biotin-labeled probes were immobilized onto the nanowires coated with the inverted Y-shaped peptides with antifouling properties. The peptide that binds tightly to the surface of the polyaniline nanowires protects the platform from nonspecific bindings. As an additional advantage, nanowires provided a larger surface area compared to the other conventional electrical wires;^{64–67} hence increasing the number of biomolecules that can be immobilized on the surface and enhancing the sensitivity of the platform by generating a more stable current signal. This biosensing platform provided a wide linear range and a LOD of 3.5 fM in serum samples.

Although antibodies are widely used as recognition elements in targeting specific COVID-19 antigens, they possess limitations such as low stability, easy degradation, and high-cost. To hurdle such obstacles, aptamer technology has been proposed as alternatives to antibodies as they present low-cost, reproducibility, and excellent stability.⁶⁸ Owing to these advantages, they have urgently implemented in electrochemical sensing devices.⁶⁹ For instance, an electrochemical dual-aptamer biosensor was developed to detect the N proteins of SARS-CoV-2. In the design, two thiol-modified aptamers were employed as recognition element, and they were immobilized on the surface of the gold electrode. Then, horseradish peroxidase (HRP) and G-quadruplex DNAzyme were coated on a metal–organic framework MIL-53(Al) decorated with Au@Pt nanoparticles in order to amplify the signal, and the platform was able to detect as low as 8.33 pg/mL in serum, holding great potential in early diagnosis of COVID-19. Yet, the system requires labeling steps to boost the signal that requires additional steps, limiting the facile use feature of this platform. Another electrochemical aptamer biosensor was developed to quantitatively measure the S proteins of SARS-CoV-2 without any labeling steps or signal amplifying agents.⁷⁰ Here, a thiol-functionalized aptamer was immobilized on a gold electrode surface, and the sensing system was able to recognize a variety of S protein concentrations in serum and artificial saliva through specific alterations in the aptamer

conformation after the binding to the S protein, thereby generating quantitative electrochemical signals within 15 s. The sensor was able to detect the presence of S protein in a clinical range; nevertheless, it possessed a lower signal gain, critically limiting its deployment to the clinical settings. Hence, the optimization of aptamer's conformational change on the matrix is essential for commercial purposes. In a similar study, a screen-printed carbon electrode platform was modified with AuNPs, which were then coated with thiol-functionalized aptamers to detect S proteins of SARS-CoV-2⁷¹ (Figure 2D). Measurements based on the electrochemical impedance spectroscopy were recorded in PBS solution containing $\text{Fe}[(\text{CN})_6]^{3-/4-}$ as a redox probe. Electron transfer in this system was enhanced by the attractions between the positively charged S-protein on the probe and the negatively charged redox species in the PBS solution. Per the proportion to the analyte concentrations, more S-proteins were captured by the aptamer–target complex. Homogeneous distributions of S proteins were first enabled on the gold electrode surface, and then, the detection of S proteins in a wide range of concentrations was conducted by electrochemical impedance spectroscopy within 40 min. The LOD was measured down to 1.30 pM or 66 pg/mL (Figure 2E,F), and moreover, this biosensor exhibited high selectivity against S proteins of SARS and MERS viruses (Figure 2G,H). However, considering the urgency and severity of the COVID-19 pandemic, lengthy assay time would need to be thoroughly decreased to implement this assay for more practical applications. It was also shown that the biosensor could be used for up to 3 weeks with a maximum activity loss of 1% compared to freshly manufactured sensors. Despite low performance reduction, the stability of aptasensors needs to be reconsidered for a long term storage. More extended stability of aptamers on a biosensor surface is required, so that the sensing device would be presumably employed as a POC device, especially in the areas with the constrained resources for COVID-19 testing. As we and the others foresee that aptamer technology will rapidly grow and further improve in the near future, more efficient oligonucleotide or peptide molecules should be designed to detect viral proteins within a shorter period of time. In the meantime, other biosensing systems that detect SARS-CoV-2 proteins in saliva within 100 ms seem more desirable for such purposes.⁷² However, this biosensor was constructed using materials such as nickel, which can be exposed to oxidation easily. This intrinsic oxidation problem needs to be controlled for more reliable measurements.⁷²

Optical Sensing Modality. Next to the electrochemical sensing mechanism, optical modalities have been utilized mostly as biosensing platforms due to their noninvasive or minimally invasive interactions with biological specimens.^{53,73–82} In this scope, the recent work on the plasmonic detection modality was able to measure SARS-CoV-2 N antibodies in unprocessed human serum within 15 min.⁸³ In this study, recombinant N proteins as recognition elements to sense anti-nucleocapsid antibodies were immobilized on a gold surface. The captured antibodies caused local changes in the refractive index and they were detected down to nM range. Moreover, unifying localized surface plasmon resonance (LSPR) sensing with plasmonic photothermal (PPT) modality has provided an alternative solution for the clinical management of COVID-19.¹ For this purpose, gold nanoislands were modified with complementary DNA sequences against a target sequence of SARS-CoV-2. Thermoplasmonic heat was

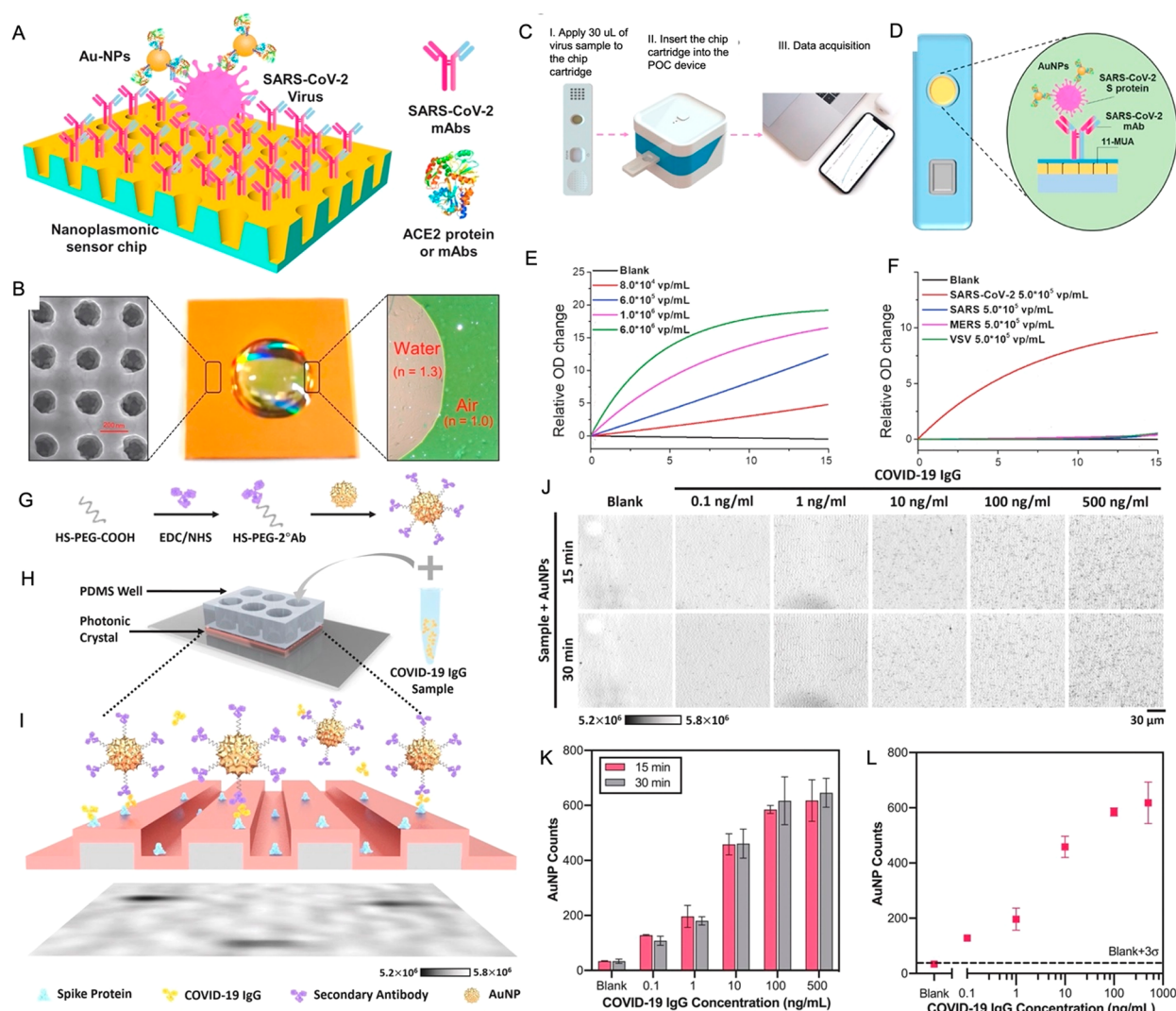


Figure 3. Optical detection of SARS-CoV-2 virus. (A) Schematic diagram of the nanoplasmonic resonance sensor for determining SARS-CoV-2 pseudovirus concentrations. (B) An image (middle) of single Au nanocup array chip with a water droplet on the surface. Scanning electron microscopy image (left) of the replicated nanocup array. Transmission microscopy image (right) of the air and water on the device surface exhibiting different colors (green and far red–pink). (C) A schematic illustration of a low-cost hand-held nanoplasmic sensor chip cartridge for the detection of SARS-CoV-2 pseudovirus. (D) The illustration presenting how the sensor chip cartridge captures specific SARS-CoV-2 viruses. (E) Dynamic binding curves obtained from the interactions between antibody and the different concentrations of the SARS-CoV-2 pseudovirus over the range $0\text{--}6.0 \times 10^6$ vp/mL. (F) Specificity analysis using different pseudoviruses of SARS-CoV-2, SARS, MERS, and VSV [Reprinted with permission from Huang, L.; Ding, L.; Zhou, J.; Chen, S.; Chen, F.; Zhao, C.; Xu, J.; Hu, W.; Ji, J.; Xu, H.; Liu, G. L. One-Step Rapid Quantification of SARS-CoV-2 Virus Particles via Low-Cost Nanoplasmic Sensors in Generic Microplate Reader and Point-of-Care Device. *Biosens. Bioelectron.* **2021**, *171*, 112685 (ref 85). Copyright 2021 Elsevier]. (G) A schematic of PRAM-based AC + DC immunoassay for the detection of human IgG against SARS-CoV-2. (I) Zoom-in view of the AC + DC immunoassay. (J) AC + DC immunoassay of serological human IgG against SARS-CoV-2. (K) Quantitative analysis of particle count for variable concentrations of COVID-19 IgG-spiked in human serum samples. (L) Quantification of AuNPs as a function of serological COVID-19 IgG concentration [Reprinted with permission from Zhao, B.; Che, C.; Wang, W.; Li, N.; Cunningham, B. T. Single-Step, Wash-Free Digital Immunoassay for Rapid Quantitative Analysis of Serological Antibody against SARS-CoV-2 by Photonic Resonator Absorption Microscopy. *Talanta* **2021**, *225*, 122004 (ref 101). Copyright 2021 Elsevier].

generated intrinsically on a local area of gold nanoislands when the light is exposed at the resonance frequency. The localized PPT heating elevated in situ hybridization temperature and facilitated proper selectivity and direct discrimination of two similar gene sequences through a mutual integration of LSPR and PPT strategies. This hybrid modality was able to detect the target sequences as low as 0.22 pM in a heterogeneous mixture. Interferometric optical detection, as another strategy, holds high potential to recognize SARS-CoV-2 immunoglobulins (IgG, IgM, and IgA) in saliva and serum samples.⁸⁴ This system basically consisted of recombinant S proteins of SARS-

CoV-2 immobilized on biophotonic sensing cells (BICELLS) as photonic transducers. Although the platform could detect S proteins, the read-out signals obtained from this system for negative patients and patients with mild symptoms did not show any statistical differences, which might result in false negatives/positives in clinical applications. Moreover, SARS-CoV-2 pseudoviruses have been detected and quantified using a nanoplasmonic sensor consisting of gold nanocup arrays⁸⁵ (Figure 3A–F). This platform provides a rapid and label-free detection strategy by modulating an optical transmission effect. Therefore, a high detection sensitivity for even small local

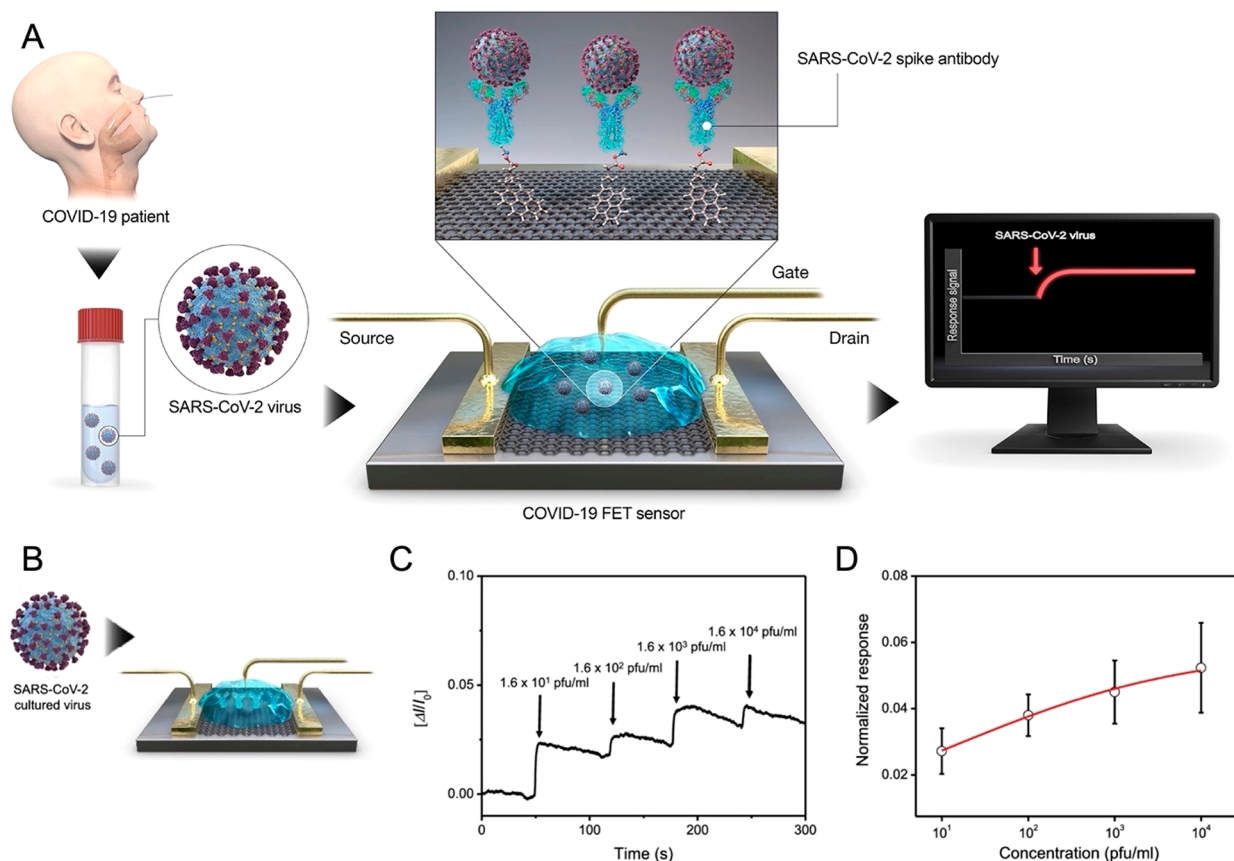


Figure 4. The detection of cultured SARS-CoV-2 virus with FET sensor. (A) A summary of procedure of COVID-19 FET sensor operation. (B) The schematic diagram of the sensor for the detection of SARS-CoV-2 particles. (C) Real-time response of the FET sensor toward the cultured SARS-CoV-2 viruses. (D) The dose-dependent response curve [Reprinted from Seo, G.; Lee, G.; Kim, M. J.; Baek, S.-H.; Choi, M.; Ku, K. B.; Lee, C.-S.; Jun, S.; Park, D.; Kim, H. G.; Kim, S.-J. S. II; Lee, J.-O.; Kim, B. T.; Park, E. C.; Kim, S.-J. S. II. Rapid Detection of COVID-19 Causative Virus (SARS-CoV-2) in Human Nasopharyngeal Swab Specimens Using Field-Effect Transistor-Based Biosensor. *ACS Nano* 2020, 14, 5135–5142 (ref 105). Copyright 2020 American Chemical Society].

refractive index changes was achieved. The readout was achieved by tracking the plasmon resonance wavelength and intensity changes on the virus-capturing sensor surface, which was functionalized with antibodies. The platform was able to detect SARS-CoV-2 pseudoviruses with a LOD of 370 vp/mL. Another label-free fiber-optic biosensing platform was developed using antibody-conjugated phase-shifted long-period fiber grating, and it was able to detect S proteins of SARS-CoV-2 in virus transport medium.⁸⁶ The constructed platform effectively measured the changes in the refractive index proportional to the concentrations of S proteins ranging from 1 to 10^8 pg/mL. Interestingly, the detection limit of this sensor showed slight variations with temperature changes, yet the measurement was shown to be highly reliable at room temperature. This variation may result in uncertainties in the measurements when employed under the temperatures out of the given ranges.

In addition to antibodies and antigens, aptamers have also been employed to optical biosensing platforms for COVID-19 diagnosis. A label-free surface plasmon resonance (SPR) aptasensor, for instance, has been manufactured to detect the N gene of SARS-CoV-2. Thiol-modified niobium carbide MXene quantum dots (Nb₂C-SH QDs) were used to construct this platform, so the aptamers targeting N genes could be anchored on the surface.⁸⁷ In the presence of this gene, aptamers were able to bind, thereby enlarging the space

between the aptamer and the chip surface, which provides a different SPR signal. The LOD of this sensor was 4.9 pg/mL, as well as it provides excellent selectivity in the presence of other respiratory viruses in human serum. In spite of what preceded, the constructed aptasensor still possessed poor repeatability, which may limit its applications in the clinical settings. This limitation would be overcome by a more stable immobilization strategy for the Nb₂C-SH QDs and aptamers on a biosensor surface. Similarly, a graphene oxide-coated optical microfiber aptasensor was also reported to detect the N proteins of SARS-CoV-2.⁸⁸ Here, RNA and DNA aptamer probes on a graphene oxide-modified optical fiber were exposed to the N protein solution at concentrations ranging from 10^{-19} to 10^{-7} M, and the spectral modulation was observed during the measurements. Upon the proportional N protein concentrations, the red-shifts in the transmission spectrum were monitored, and several concentrations were able to be recognized with a high linearity. In view of this strategy, spreading graphene oxide on the fiber surface increased the surface-to-volume ratio, creating a larger area for aptamer immobilization, thereby resulting in a lower LOD (6.25×10^{-19} M) for the detection of N proteins in serum, as well as providing a short turnover (around 3 min). Unfortunately, in the setup, the optical microfiber exhibited certain fragility, and the antibody attached to the fiber may be easily saturated, thereby reducing the sensing efficiency.

In addition, microfluidics as an integrated technology has significantly improved the outcomes of many biomedical approaches, including optical biosensors for COVID-19 diagnosis through the improvements in molecular interactions between analytes and recognition elements, and also, the reductions in the thickness of the boundary layer.^{49,89–99} For this purpose, a biosensor was developed by combining an all-fiber optical system, a multimode fiber bioprobe, and a microfluidic chip.¹⁰⁰ The detection was carried out through the Fresnel reflection mechanism coupled with an immunoassay strategy. The single-multimode fiber optic coupler used in this system simplifies the optical structure of the Fresnel reflection on the biosensor, and also enables a label-free testing of targets in nanoliter volumes. Apart from this, it has caused the transmission efficiency of incident and reflection light to increase to a great extent, thereby improving the sensitivity. IgM and IgG antibodies against S protein of SARS-CoV-2 was recognized less than 7 min, and the platform achieved detection down to 0.82 and 0.45 ng/mL for IgM and IgG, respectively.

Another limitation for the utility of these sensors to the field or bedside is multiple washing steps. In this manner, a single-step, wash-free procedure was applied on a photonic crystal biosensor to detect IgG against SARS-CoV-2 using only a single droplet of serum¹⁰¹ (Figure 3G–L). The surface of the photonic crystal was coated with the S proteins of SARS-CoV-2, forming a sandwich-like immunocomplex that involved antibody-modified AuNPs, IgG, and S proteins. Using such a sensing device, an LOD of 100 pg/mL and an assay time of 15 min were achieved. In the near future, such improvements in practicality would be one of the most crucial steps for the deployment of sensors to settings requiring limited training and resources.

Field-Effect Transistor Biosensors. Researchers in the realm of advanced materials have been attempting to find out new solutions to circumvent current drawbacks faced in gold standard methods. Unprecedented features of advanced materials have enabled us to reach sensing low concentrations of biotargets, potentially addressing some crucial challenges in outdated, bulky platforms. Viewed in this way, a field-effect transistor (FET) based sensing system has emerged to overcome the drawbacks of available sensing technologies. Briefly, FET is a type of transistor that utilizes an electric field to control the current flow, so weak-signals can be amplified.¹⁰² Particularly, in the shadow of the COVID-19 pandemic, FET-based semiconducting two-dimensional materials have drawn attention as a potential candidate for rapid and label-free detection of SARS-CoV-2. Graphene, for instance, is a single layer, atomically flat, and hexagonally arranged carbon atom sheet.¹⁰³ The specific binding of biological agents on graphene surfaces is mostly measured in terms of various electrical parameters, including alterations in current, resistance, or impedance changes.¹⁰⁴ Researchers have devoted great effort and many resources to graphene derivatives in developing such systems. In this regard, a FET-based sensing system was constructed to detect SARS-CoV-2 in nasopharyngeal swab samples directly¹⁰⁵ (Figure 4). The sensor was designed on graphene sheets considering the detection mechanism through FETs, and the sensor surface was then decorated with specific antibodies against the S proteins. During the measurements, the biosensor was operated under physiological buffer conditions as an electrolyte matrix to maintain an efficient gating effect. The buffer solution gated FET system was able to

detect viruses by measuring the changes in the channel surface potential and the corresponding effects on the electrical response. The system enabled the detection of antigens down to 1 fg/mL in PBS and 100 fg/mL in clinical transport medium. This system was further adapted to detect intact viruses as low as 1.6×10^1 pfu/mL and 2.42×10^2 copies/mL from culture media and nasopharyngeal swab specimens, respectively. With the presented configuration, there was no longer sample pretreatment or labeling steps in detecting SARS-CoV-2. Furthermore, another graphene-FET sensor was able to measure the amount of SARS-CoV-2 S protein S1 as low as 0.2 pM within 2 min without any labeling procedures.¹⁰⁶ Further developments on this sensor were employed to monitor antibodies with a high binding constant ($2 \times 10^{11} \text{ M}^{-1}$) against the receptor-binding domain with a low concentration (0.1 pM). This sensor hence provided an attractive alternative to the examination and rational design of neutralizing antibody locking approaches for this continuing malady and its use for screening and early diagnosis. Reduced graphene oxide has also been used to fabricate silicon-based FET biosensors for SARS-CoV-2 detection.¹⁰⁷ Briefly, the constructed FET was functionalized with amine groups on the graphene surface through APTES to immobilize monoclonal anti-SARS-CoV-2 antibodies (mAbs). When a negatively charged antigen binds to the surface, the depletion of charge carrier causes a reduction in electrical conductivity and discharge current. Similarly, the binding of a positively charged protein leads to an increase in conductivity. Through this strategy, the platform was able to detect down to 0.002 fM in samples acquired through nasal swab. In a different study, graphene was modified with phosphorodiamidate morpholino oligo (PMO) probes to construct an FET nanosensor for the detection of SARS-CoV-2 RNA in human throat swab specimens.¹⁰⁸ The surface of graphene was immobilized with AuNPs, which were then conjugated with PMO probes. Leveraging a high surface-to-volume ratio, the high stability of AuNPs, and the efficiency of the PMO probe, the low amounts of SARS-CoV-2 RdRp gene could lead to a measurable shift in the Dirac point of the FET sensor through the probe hybridization. Within 2 min, the nanosensor provided accurate results down to 0.37, 2.29, and 3.99 fM in PBS, throat swab, and serum, respectively. Moreover, a single nanosensor was capable of analyzing RNA extracts from 30 different clinical samples. To put it concisely, despite the fact that the reported sensors were shown to be effective in COVID-19 diagnosis, novel materials to integrate with FET biosensors are required to reduce noise signals and increase their precision.

Although graphene-based materials are currently more attractive for the FET systems, other semiconductive materials have been also employed in the design of such COVID-19 diagnosing devices. A tungsten diselenide (WSe_2)-based FET system was recently fabricated for the rapid and sensitive detection of SARS-CoV-2 in vitro.¹⁰⁹ Accordingly, the WSe_2 crystal monolayer was functionalized with a mAb against the S protein of SARS-CoV-2. The platform sensed the levels of S proteins down to 25 fg/ μL and it only required 8 μL of sample prepared in 0.01X PBS. Due to the existing difficulties in the fabrication techniques of this platform, batch-to-batch variations would impede the signal quality and reliability of the platform. Moreover, single-walled carbon nanotubes (SWCNTs) were shown to reduce the assay cost and offer higher analytical sensitivity toward the target analyte compared to graphene-based counterparts.¹¹⁰ An SWCNT-based FET,

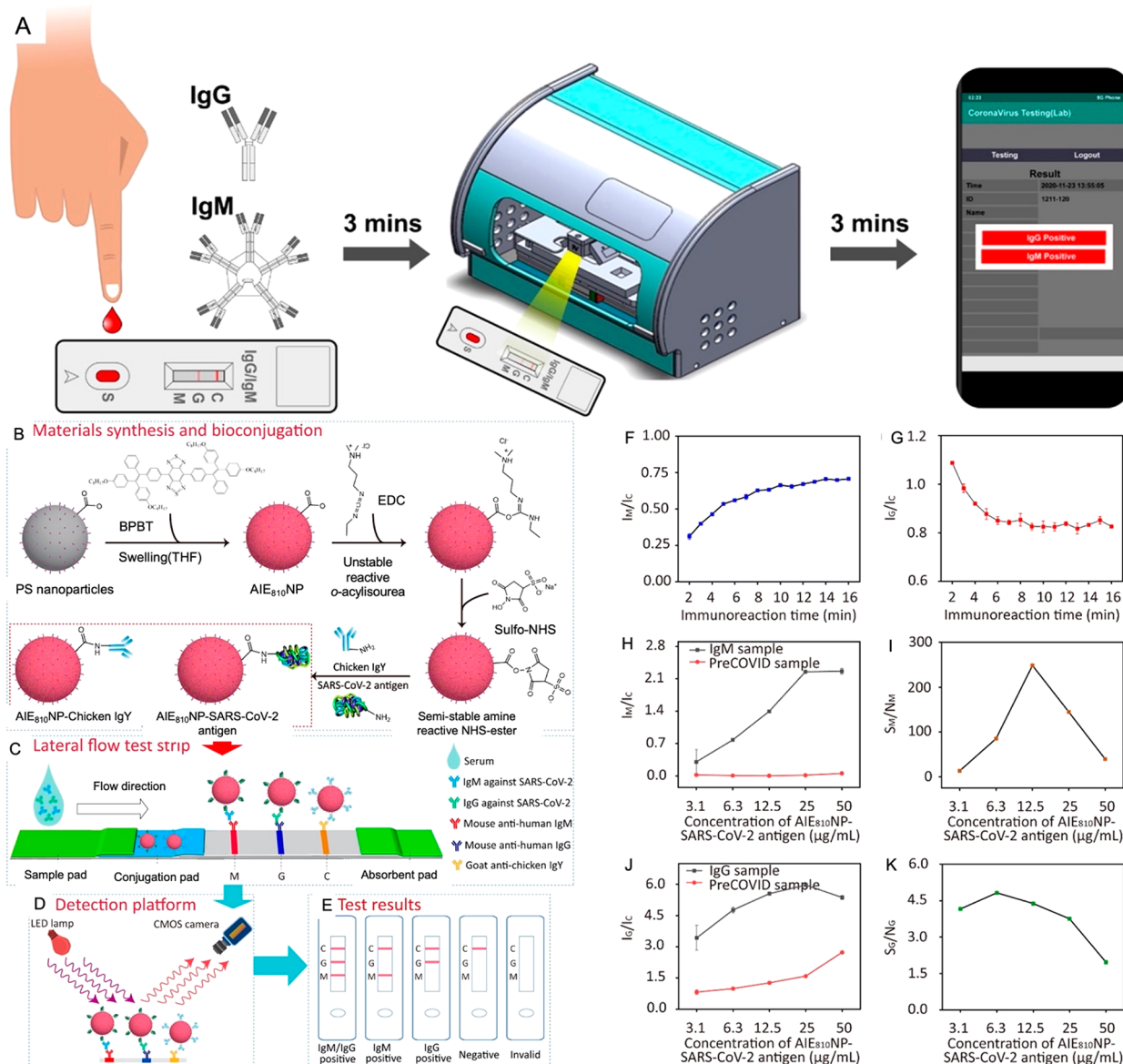


Figure 5. (A) The workflow of quantitative spectral LFIA platform. The optical-based platform utilizes 10–20 μL of blood from a fingertip or a vein to the test strip, integrating the immunoglobulins and producing results in 5–10 min [Reprinted with permission from Chen, P.-Y.; Ko, C.-H.; Wang, C. J.; Chen, C.-W.; Chiu, W.-H.; Hong, C.; Cheng, H.-M.; Wang, I.-J. The Early Detection of Immunoglobulins via Optical-Based Lateral Flow Immunoassay Platform in COVID-19 Pandemic. *PLOS One* 2021, 16, 1–13 (ref 118) Copyright 2021 PLOS One. (B–K) Schematic illustration of the NIR-emissive AIE nanoparticle-labeled lateral flow immunoassay for detection of IgM and IgG [Reprinted from Chen, R.; Ren, C.; Liu, M.; Ge, X.; Qu, M.; Zhou, X.; Liang, M.; Liu, Y.; Li. Early Detection of SARS-CoV-2 Seroconversion in Humans with Aggregation-Induced Near-Infrared Emission Nanoparticle-Labeled Lateral Flow Immunoassay. *ACS Nano* 2021, 15, 8996–9004 (ref 132). Copyright 2021 American Chemical Society].

for instance, was functionalized with anti-SARS-CoV-2 S and N protein antibodies for monitoring the concentrations of SARS-CoV-2 antigens in clinical nasopharyngeal samples.¹¹¹ Here, an SWCNT monolayer was deposited over the patterned AuNPs to decorate antibodies onto the surface. The high purity of SWCNTs offered high state conductivity and high on/off ratios for the FETs, improving the analytical sensitivity of this system. A small volume of sample (2 μL) was applied to the sensor and incubated for 2 min. Within such a short assay time, the platform was capable of detecting as low as 0.55 and 0.016 fg/mL of S and N proteins, respectively. In summary, FET biosensors hold great potential as rapid screening tools. When combined with 2D semiconducting materials, this

modality could be utilized to identify SARS-CoV-2 infected individuals rapidly from a minute volume of samples.

Lateral Flow Assays. In addition to the aforementioned sensors, LFAs have been extensively employed to COVID-19 diagnosis, providing an important impact as an alternative to the techniques that heavily depend on laboratory facilities.¹¹² Highlighting again, LFA is a facile, low-cost, and portable paper-based platform, where the sample from a patient is simply placed on the device and the operator who has limited training receives the assay results within a very short period of assay time. In principle, LFAs can be classified according to recognition elements employed on the platform. Lateral flow immunoassays (LFIAs), in which antibodies are used as a

recognition element, have been widely studied, and different LFIA systems have been designed for early diagnosis of COVID-19.¹¹³

On the other hand, nanoparticles are thoroughly utilized in such systems as they enhance the visibility of the results and stability of the LFIA systems. As an example, SARS-CoV-2 N proteins were immobilized to the surface of the strip of the LFIA system, so antibodies against the N protein were captured on the surface and further coupled with IgG-conjugated AuNPs for the signaling.¹¹⁴ Detecting these proteins from a volume of 80 μL took around 15–20 min. Moreover, two major parameters, i.e., the concentration of coating antigen and pH value, were found to be key factors that interfere with the reliability of the sensor. Similarly, another AuNP-based LFIA platform was integrated with a multiplex reverse transcription loop-mediated isothermal amplification for the detection of SARS-CoV-2 RdRp and N genes from patient samples.¹¹⁵ The LOD of this sensor was as low as 20 copies per reaction. In addition, the entire process consisting of reaction preparation, viral RNA extraction, and sample analysis could be achieved within 80 min, which is faster than that of the existing RT-PCR methods (~ 150 min). The total running cost of one test was approximately \$6.50, which was considerably high for an LFIA. The overall cost of this test should be reduced to compete with its counterparts; it should also be reduced to compete with RT-PCR tests, which were reported to be roughly \$7.¹¹⁵ Another AuNP-based LFIA with optical and chemiluminescence settings was developed to detect IgA levels in saliva (9 samples), and also, IgG and IgM levels in serum (25 samples). Importantly, it was the first study ever reported to detect IgA in saliva, and the turnaround assay time was about 15 min.¹¹⁶ Due to the paucity of information regarding the clinical role of salivary IgA and its correlation in serum for the COVID-19 infection,¹¹⁷ such a sensor system may fail in determining infection stages; hence, additional efforts in molecular analyses are required to make a conversation between salivary and serum concentrations of IgA. A similar optical LFIA platform was designed using AuNPs to detect IgM and IgG in 111 participants, who were suspected of having COVID-19 infection¹¹⁸ (Figure 5A). Using 10–20 μL of blood from a finger prick or a venipuncture enabled results in less than 10 min. AuNPs were also integrated into a microfluidic-integrated LFIA sensing platform to detect RNA molecules of SARS-CoV-2 in 37 positive and 17 negative clinical samples collected by throat-nasopharyngeal swabs.¹¹⁹ First, amplification products labeled with fluorescein amidite (FAM) and biotin bound to the gold-labeled FAM-specific antibodies on the conjugation pad. The bound amplicons then flowed through a capillary action into the test strip channel, which was precoated with biotin-ligands, forming a sandwich detection strategy. Amplicons that captured only gold-labeled antibodies, bound to the immobilized biotin-ligand molecules, resulting in a red color band-signal. The assay was completed within 30 min, along with an LOD down to one copy per μL (considering 30 μL of sample volume, it is around 30 copies per sample). The sensitivity and specificity were 97% and 100%, respectively, and these results were highly comparable to the current PCR-based diagnostic tools.

As stated above and further described in other reports,^{120–125} most of the LFA platforms were constructed using AuNPs. As alternatives, other nanoparticles have also been integrated with LFIA systems. As an example, an LFIA reliant on the lanthanide-doped polystyrene nanoparticles was developed to determine anti-SARS-CoV-2 IgG in serum samples.¹²⁶ A

recombinant N phosphoprotein of SARS-CoV-2 was principally dispensed onto a nitrocellulose membrane, followed by the accumulation of mouse antihuman IgG antibody labeled with lanthanide-doped polystyrene nanoparticles, forming a visual signal within 10 min. The assay was validated as a small cohort validation with 7 patient samples collected from RT-PCR positive individuals and 12 samples from RT-PCR negative individuals who were considered to be clinically suspicious. One of the negative samples resulted in a SARS-CoV-2 IgG positive result, while the outcomes for the other samples were coherent with those reached via RT-PCR. Quantum-dot nanobeads were also employed as a luminescent label in LFIA to enhance the signals during the detection of viral antigens in serum samples.¹²⁷ LFIA was constructed by conjugating SARS-CoV-2 S proteins and nanobeads on each antigen-binding site of an antibody to form a double-antigen sandwich, confirming the presence of COVID-19 infection in patients. Compared to the AuNP-based LFIA systems, the turnaround time was approximately 15 min, and the platform provided 100% specificity. The designed platform presented some limitations in terms of portability due to the requirement for a fluorescent reader—a specially configured system for this study, which restricts its expansion to larger geographies for COVID-19 detection. Quantum-dot nanobeads have also been utilized for enhancing the efficiency of LFIA platforms in detecting IgM and IgG against SARS-CoV-2 from 57 human serum samples.¹²⁸ Here, the quantum-dot nanobeads were further conjugated with SiO_2 and AuNPs as the labeling strategy. The assay required only 1 μL of serum sample and provided a result in less than 15 min. The sensing platform proved to be 100 times more sensitive compared to the platforms containing only AuNPs. However, using quantum-dots in such systems faces severe limitations due to their extremely small size (5–20 nm), and therefore, they are challenging to centrifuge using a conventional system. Moreover, chemical modifications to these systems are highly challenging, and they usually require an additional UV light source for fluorescent signal measurements.

Polymersomes are artificial hollow-shell nanoparticles formed by the self-assembly of amphiphilic block copolymers, and they are widely used to encapsulate bioactive molecules.¹²⁹ As an interesting example, they have been utilized to encapsulate dyes to design a naked-eye detection in samples obtained from 61 serums and 60 nasal swabs.¹³⁰ This nanodiagnostic LFIA platform demonstrated a sensitivity of >90% for both antigen and antibody tests. With a reproducibility of 96–98%, the platform provided accurate diagnosis (91–97%) after 4 weeks. Indeed, this sensing system was shown to suffer from limitations regarding the sensitivity compared to the RT-PCR technique. As the study involved a sample group containing only one sample with low virus load, the platform still needs some improvements for larger cohorts. Polymer nanoparticles were also included in the LFIA platform for the detection of ORF1ab and nucleoprotein genes of SARS-CoV-2 from the swab samples.¹³¹ Briefly, nanoparticles were coated with streptavidin, and the accumulation of nanoparticles led to a band with crimson color in the presence of SARS-CoV-2. The LFIA was then coupled with a multiplex reverse transcription loop-mediated isothermal amplification system and provided a detection down to 12 copies per reaction. Both sensitivity and specificity of the assay were 100%, and the assay was completed within an hour. The study was also conducted with a small number of clinical samples

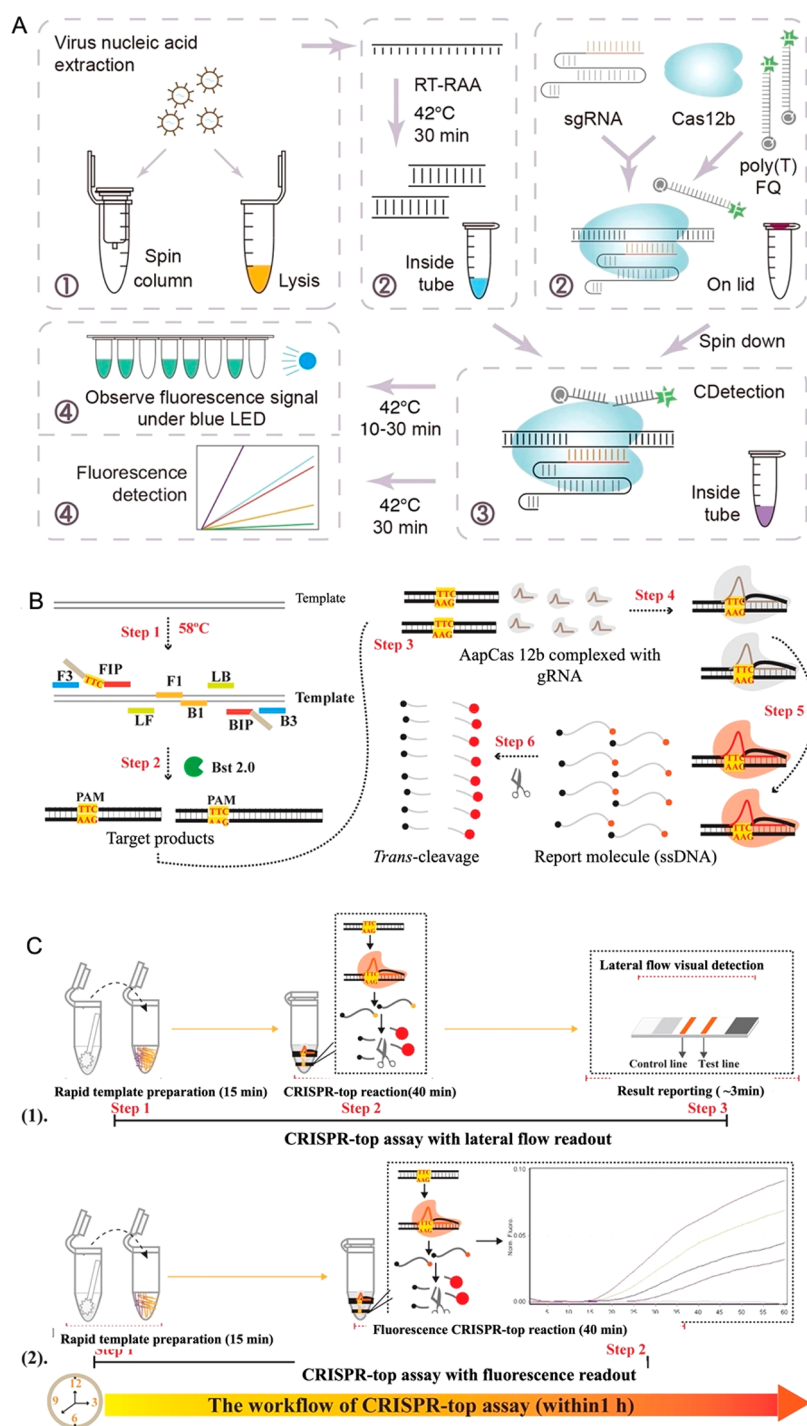


Figure 6. A schematic showing the workflow of CASdetec [Reprinted with permission from Guo, L.; Sun, X.; Wang, X.; Liang, C.; Jiang, H.; Gao, Q.; Dai, M.; Qu, B.; Fang, S.; Mao, Y.; Chen, Y.; Feng, G.; Gu, Q.; Wang, L.; Wang, R. R.; Zhou, Q.; Li, W. SARS-CoV-2 Detection with CRISPR Diagnostics. *Cell Discov.* 2020, 6, 1–4 (ref 143). Copyright 2020 Macmillan Publishers Ltd.: NATURE. (B–C) An outline of the CRISPR-top design [Reprinted with permission from Li, S.; Huang, J.; Ren, L.; Jiang, W.; Wang, M.; Zhuang, L.; Zheng, Q.; Yang, R.; Zeng, Y.; Luu, L. D. W. A One-Step, One-Pot CRISPR Nucleic Acid Detection Platform (CRISPR-Top): Application for the Diagnosis of COVID-19. *Talanta* 2021, 233, 122591 (ref 146). Copyright 2021 Elsevier].

collected from the oropharyngeal area. The feasibility of the assay needs to be further evaluated using different types of specimens collected from the other clinical samples, such as nasopharyngeal swabs.

The use of nanoparticles as fluorescent reporters has also been employed. Accordingly, polystyrene nanoparticles were designed for a strategy of aggregation-induced emission (AIE)

and used as reporters in LFIA to monitor the concentrations of IgM and IgG against SARS-CoV-2¹³² (Figure 5B–K). To further amplify the fluorescent labeling signal, the ligand was labeled with a 300 nm of polystyrene nanoparticles loaded with 3.18×10^6 dye (AIE810NP). Using the near-infrared (NIR) emission of the AIE810NP as the detection signal efficiently eliminated possible autofluorescent interference from the

membrane, thereby improving the sensitivity and any noise of the lateral LFIA. Normally, detecting IgM and IgG levels with AuNPs has been reported to be between 8 and 15 days after symptom onset, and using AIE nanoparticles, this period was further reduced to 1–7 days according to a validation study composed of 172 serum samples. Additionally, the LODs were 0.236 and 0.125 $\mu\text{g/mL}$ for IgM and IgG, respectively. The sensitivity values of the proposed LFIA were 78% for IgM and 95% for IgG, which were higher than those of the commercial AuNP-based test strips (41% for IgM and 85% IgG). Similarly, the QIArearch LFIA system from QIAGEN reliant on the use of fluorescent nanoparticles was constructed to detect IgG, IgM, and IgA concentrations in plasma samples.¹³³ The platform provided results in 3–10 min with 93.85% of sensitivity and 97.83% of specificity.

A novel surface-enhanced Raman scattering-based LFIA was reported for the simultaneous detection of anti-SARS-CoV-2 IgM and IgG in 19 serum samples from COVID-19 positive and 49 serum samples from COVID-19 negative patients.¹³⁴ The required tags to detect immunoglobulins were decorated on a core–shell structure (Ag shell@SiO₂ core). The synthesized core was further modified with S proteins to recognize immunoglobulins, and this platform improved the detection limits 800 times better than that of standard AuNP-based LFIA owing to implementing Raman-based detecting modality.

Clustered Regularly Interspaced Short Palindromic Repeats Strategy. The clustered regularly interspaced short palindromic repeats (CRISPR) and CRISPR-associated (Cas) genes generate RNA-guided genome defense systems that ensure adaptive immunity to external genetic elements in bacteria.¹³⁵ The discovery of CRISPR/Cas has revolutionized biology and created new horizons for molecular medicine. In principle, genetic materials (DNA or RNA) can be regulated precisely through this strategy, and more recently, deploying CRISPR/Cas systems to in vitro detection strategies has highlighted an innovative, powerful, and precise framework in the existing area of molecular diagnostic platforms.^{136–138} Not limited to these aspects, this strategy is now widely applied to many areas, for instance fundamental research, drug development, fuel production, and human genome engineering against certain diseases.

Hitherto, a series of nucleic acid amplification assays have been integrated with CRISPR type strategies for SARS-CoV-2 detection,¹³⁹ including isothermal nucleic acid amplification tests (e.g., loop-mediated isothermal amplification (LAMP)) that require only one temperature, accelerating the access of PCR amplification at resource-constrained settings.¹⁴⁰ Considering the drawbacks in the gold standard method detailed in the section **Current Platforms for COVID-19 Diagnosis**, CRISPR-based applications have provided facile and time-saving alternatives to the existing systems for SARS-CoV-2 detection.^{141,142} CRISPR-Cas12b-based DNA detection (CAS-detec), for instance, was reported to identify SARS-CoV-2 viral particles¹⁴³ (Figure 6A). This detection platform, combining sample pretreatment and nucleic acid amplification methods, provided no cross-reactivity, and it was capable of detecting as low as 10⁴ viral copies/mL. In order to possess high sensitivity, specificity, and availability, a colorimetric method based on the CRISPR/Cas12a system was developed for the detection of SARS-CoV-2 in a recent study.¹⁸⁴ With this method, SARS-CoV-2 RNA from synthetic sequences and the cultured viruses

can be detected with the naked eye based on AuNP-integrated probes, down to 50 RNA copies per reaction.

Comprehensive integrations into portable platforms have made possible the utilization of CRISPR Cas12-based systems. Their integration with a standard plate reader and paper strip assays, for instance, was adapted in two different detection methods, and it also enabled lower LODs, which were even smaller than the minimum levels at conventional methods to determine the level of viruses in clinical samples.¹³⁷ With such a platform, the researchers demonstrated a portable and affordable (\$1–2) platform, detecting synthetic RNA fragments of SARS-CoV-2 corresponding to ORF1ab, ORF1b, and RdRp genes, which were included using the WH-human1 sequence (GenBank MN908947). Spectrometric measurements on a standard plate reader depicted a low LOD value of ORF1ab SARS-CoV-2 down to 10 copies/ μL . Similarly, a paper strip version of this strategy provided comparable performance in terms of detection, indicating an important utility of CRISPR-Cas12 detection technology that does not require a bulky and costly instrument. On a parallel track, another CRISPR-Cas 12-stemmed LFA was validated with samples extracted from respiratory swabs.¹⁴⁴ In addition, a CRISPR-based nucleic acid detection strategy was developed on an LFA and further modified with fluorescent markers for higher sensitivity.¹⁴² The assay was validated with 60+ virus species and their subspecies, such as SARS-CoV-2 and other phylogenetically closer virus types. Ultimately, the platform was able to identify synthetic SARS-CoV-2 RNA as low as 10 copies/ μL .

Unifying reverse transcription and LAMP, target sequences of E and N genes of SARS-CoV-2 were amplified at an isothermal temperature (62 °C) within 20–30 min, and the Cas12 detection was confirmed at 37 °C for 10 min. The DNA endonuclease-targeted CRISPR trans reporter (DETECTR) assay provided a naked-eye detection on an LFA strip within 30–40 min. The SHERLOCK (specific high sensitivity enzymatic reporter unlocking) method, another CRISPR-mediated method, demonstrated an alternative approach by combining isothermal amplification with CRISPR that facilitates existing the CRISPR procedures and implements them into wider settings, where there is a lack of the expensive equipment and reagents required in qRT-PCR. In particular, STOPCOVID (SHERLOCK testing in one pot) was able to obtain 100 SARS-CoV-2 viral genomes in saliva and nasopharyngeal swabs within an hour. This platform was also comprehensively validated with 12 positive and 5 negative patient samples and provided similar results to the conventional tests.¹⁴⁵ The integration of CRISPR and target gene preamplification in the same system also decreased the cross-contamination of samples. Taking this advantage, another CRISPR-mediated method was developed to detect SARS-CoV-2, which was performed in a single reaction mixture¹⁴⁶ (Figure 6B,C). The system targeting the ORF1ab and NP genes was able to provide visually interpretable results in about 60 min and detected down to 10 copies per reaction without any cross-reactivity. Similarly, a four-step procedure including RNA extraction, multiple cross displacement amplification, CRISPR/Cas12/CrRNA detection, and LFA was conducted in a total analysis time of 60 min,¹⁴⁷ and this strategy was capable of detecting 7 copies per reaction.

It is noteworthy that the CRISPR-originated LFA platforms result in a shorter turnaround time, and also, they do not require any sophisticated instrumentation compared to the

conventional assays, leveraging their accessibility and further implementation to the settings, lacking significant amount/sophisticated level of resources.¹⁴⁸

■ FUTURE DIRECTIONS AND INTEGRATION OF OTHER TECHNOLOGIES

COVID-19 has spread to a large geographic area due to its strong infectivity and difficulties in the current detection systems, and eventually, it led to a sudden and rapidly developing outbreak. Moreover, we require the use of geographic information systems and big data technology to provide new solutions in rapid analysis that can take necessary actions to prevent and control the outbreak dynamics.¹⁴⁹ In recent years, there have been enormous developments in Artificial Intelligence (AI) and machine learning along with the internet of things (IoT). Thus, there are technological developments that will have many effects in the field of health, as well as daily activities such as social media, e-mail, web searches, passport services, travel cards, shopping, and park services.¹⁵⁰ In March 2020, the White House, in collaboration with some companies and research institutes, urged global AI researchers to act for developing new strategies and techniques to assist the research on COVID-19. For instance, the Allen Institute, together with the partnership of leading research groups on AI, has launched an open-source COVID-19 Open Research Dataset that constantly publishes academic publications up-to-date. In this manner, a platform has been created to accelerate new research projects that require real-time results. The large-scale outcomes of COVID-19 patients could be examined via innovative machine learning algorithms, and these analyses could provide a viral spread model, further improving the existing diagnostic strategies and foreseeing potential diagnostic opportunities, as well as guiding new therapeutic approaches.¹⁵¹

Worldwide, governments and healthcare officials have been working to curb the COVID-19 outbreak, protect people, and restore social order. Technology companies have also contributed to the fight against the pandemic and they have saved lives with the tools that they have developed or adapted. Google and Apple, for instance, have started collaborating to ensure that governments and healthcare organizations use Bluetooth technology with user privacy and security during the introduction of such technologies. Since SARS-CoV-2 can be transmitted through close contact with infected people, public health services are thought to be a valuable tool to help control the spread of the disease. These companies have been preparing a wide-ranging solution that contains application programming interfaces and operating system-level technology to enable contact tracking.¹⁵²

In Silico Models to Curb the Pandemic. To develop a rapid clinical intervention through diagnosis and treatment strategies, it is necessary to know any possible changes in viral structure and genome in the same family.¹⁵³ At first glance, computational approaches have been deployed to seek potential therapeutics and vaccines against SARS-CoV-2 entry to the host cells and/or enhancing immune response for the infection. Coronavirus infection has occurred with serious symptoms in both humans and animals the last two decades. Tilocca et al. performed an *in silico* study of major N protein epitopes with taxonomically linked coronavirus homologues for animal species, closely related to the human population. A high sequence homology was observed for some proteins. Structural epitope mapping results revealed a

potential immunogenic effect for specific sequences that shows a lower identity with the N proteins of SARS-CoV-2.¹⁵⁴ In addition to these efforts, the investigation of post-translational modifications and the three-dimensional structures of viral proteins included in host–pathogen interactions provides convenience during the fight against infection.¹⁵⁵ In this manner, O-glycosylation and phosphorylation positions were determined by employing the full sequence of amino acid of the S1 protein of SARS-CoV-2, followed by multiple kinetic and biochemical analyses including solvent accessibility, enzyme binding activity, and evaluating surface area parameters. Accordingly, the full 3D glycoprotein structure of the S1 protein was designed by applying the carbohydrate force field with a high accuracy. Moreover, the interactions between C-type lectin and α -mannose residues were investigated profoundly, and the positions of carbohydrate recognition sites were estimated, hence providing pivotal target points to prevent SARS-CoV-2 S1 protein binding to the host.

On the other hand, instead of developing drugs from scratch, drug repurposing is another strategy, providing a solution in a shorter time of research. For instance, after systematically analyzing all the proteins encoded by SARS-CoV-2 genes, Wu et al. cross-checked them with proteins found in other coronaviruses and constructed 19 structures using homology modeling through the molecular estimation studies.¹⁵⁶ At this point, they scanned 21 targets, including 2 human targets, using the ZINC drug and their natural products databases, with targeted virtual ligand scanning. The structure and screening results of critical targets like RNA-dependent RNA polymerase, 3-chymotrypsin-like protease, and papain-like protease have been investigated. Accordingly, a database of 78 commercially available antiviral drugs has been repurposed for the treatment. In addition to the studies mentioned above, peptide inhibitors have been designed and simulated to prevent the viral entry to the host.¹⁵⁷ Inhibitors mostly consist of two consecutive α -helix structures extracted from the protease region of ACE2. Through molecular dynamic simulations, α -helix peptides have retained their secondary structure and provided an extremely stable and specific binding to SARS-CoV-2. As suggested in this report,¹⁵⁷ these peptide inhibitors would be integrated with nanoparticle carriers that bind to viral receptors, thereby designing simple and effective therapeutics against the infection. In another study, 61 molecules that are currently being used as antiviral agents were examined by docking analysis.¹⁵⁸ Per the results, 37 of these molecules were discovered, and they interact with two protein structures of SARS-CoV-2. Between the molecules reported, RNA-dependent RNA polymerase and HIV protease inhibitors showed auspicious properties for binding to the SARS-CoV-2 enzymes. Additionally, methisazone (protein synthesis inhibitor), CGP42112A (angiotensin AT2 receptor agonist), and ABT450, (nonstructural protein 3-4A) could also be appropriate treatment alternatives against COVID-19 infection. Recently, in a study aimed to prohibit the virus from entering and maturing in host cells, a homology modeling of the human TMPRSS2 enzyme, the virtual screening approach, molecular splicing study, and absorption, distribution, metabolism, excretion, and toxicity (ADMET) profile analyses have been employed to determine new and possible inhibitors against the virus.¹⁵⁹ According to the results, four commercially available drugs and four novel compounds were found as potential inhibitors of TMPRSS2 and Mpro (main protease enzyme of coronavirus). These compounds, which

were defined as drug-like compounds and displayed innocent ADMET features, were thought to help develop and optimize more productive and powerful inhibitors against COVID-19 infection.

Such *in silico* investigations have also paved the way to design and produce new prevention strategies before performing *in vitro* and *in vivo* studies, and thereby, they reduce time, effort, and cost in drug discovery research. Concurrently, all these strategies provide solutions in the area of treatment. Still, they have also constituted a basis to strategize diagnostic approaches, focusing on genetic material, serological aspects, viral surface proteins, any possible biomarkers, and initial production of viral peptides in circulation or other biospecimens.

Internet of Things: Expanding the Geography for Data Collection/Analysis during the COVID-19 Diagnosis Using Secure Cloud Settings. Mobile phones with an embedded global positioning system (GPS) are connected to mobile networks through base stations employing different generation cellular mobile communication, such as the global system for mobile communication (2G), universal mobile telecommunications system (3G), or long-term evolution (LTE). Therefore, connecting cost-effective and facile POC devices to phones, which can provide diagnostic strategies over a mobile network, will have largely benefitted from the IoT as a pivotal tool for tracking any infectious diseases and dealing with an epidemic/pandemic.¹⁶⁰ Technological advances like fog and edge computing, IoT, and big data have a significant impact because of their sturdiness and capability to offer varied response characteristics based on applications.¹⁶¹ Like this, IoT refers to a network of smart devices and individuals, where data can be collected in raw form and transmitted over the internet for analysis in terms of patterns. When infrastructures such as smartphones, internet access, microneedles for sampling and injection purposes, and wearable technologies are available, such technology can help control the outbreak by collecting and analyzing data already available.^{162–164} As the pandemic of COVID-19 began to spread rapidly, cities started to apply quarantine, which brought the majority of people to stay at home. The increasing need for medical equipment and supplies has been challenging, likely exceeding the capacity for rapid, yet critically required replenishment. Individuals with mild or suspicious symptoms need to reach medical centers for further investigation on their status, and this load results in an unexpected and uncontrollable accumulation in medical centers. Such technologies hence could help accelerate diagnostic tests at the PON settings and also enable clinical management in remote settings.¹⁶⁵

Akin to similar approaches, IoT strategies have employed the drones to provide observation to enforce quarantine and mask use. This technology has been also utilized to trace the origin of an outbreak by detecting people who come into contact with patients. Hence, patients can be ensured to comply with the quarantine and the violating patients can be tracked. Similarly, this technology can also be favorable in reducing the workload of caregivers by remote monitoring of patients at their home.¹⁶⁶

Artificial Intelligence Technologies and Strategies: Standardizing Test Results and Significantly Reducing the Workload in the Clinic. The use of AI in detecting infected people leads to a remarkable revolution in health systems and medical practices. Machine learning models are basically designed to examine medical images for detecting a

disease in the early stages. Recently, the use of AI in visual tasks in medicine has increased significantly.¹⁶⁷ During the pandemic, real-time results generated around the world have been studied devotedly by scientists working on machine learning and AI. An easy-to-access data transformation is extremely vital after the timely transmission of data, such as symptoms and treatment results collected from COVID-19 patients.¹⁵¹ As a striking example, in China, where the outbreak started, studies are underway to mark those infected by SARS-CoV-2 using sensors to collect data between cities. Thanks to AI strategies, reaching computed tomography (CT) scan results in a notable reduction from 15 min to 10 s. As another instance, an AI-supported body temperature scanning system has been developed to detect very high or low temperatures in order to identify infected people in public transport.¹⁶⁸ AI algorithms can also be used as a first screening tool for suspicious cases, such as those who have traveled to countries where the outbreak is prevalent. Likewise, necessary laboratory tests can be performed for patients at high risk and their isolation can be controlled properly.¹⁶⁹ AI and machine learning can be combined with cloud, block chain, and speech recognition, creating more reliable, rapid, and secure remote monitoring system between the caregivers and the individuals.¹⁶²

To provide prompt clinical decision support, the researchers, for instance, developed a model within the AI framework using predictive analytical features and validated with real patient samples.¹⁷⁰ To this end, they have been working on fabricating a device with AI abilities that algorithmically identifies the combinations of clinical features of the disease, predicting outcomes, and giving notice to the patients at risk of more vigorous disease at the first admission. The models predict the acute respiratory distress syndrome encountered in the patients infected with COVID-19 using historical data. With the results derived from two hospitals in China, the late development of acute respiratory distress syndrome (ARDS) was predicted in the initial phase of COVID-19, leading to a slightly elevated alanine aminotransferase value, the presence of body pain, and a high hemoglobin value. Serious cases can be estimated with 70–80% accuracy with the models learned using the historical data. As shown in these recent studies, AI holds great potential to predict the outbreak and eventually minimize or stop the spread of the outbreaks, as well as optimize the clinical trials for drugs and vaccines.¹⁶⁶

Wearable Platforms and Mobile Phone Systems: Adaptation of Platforms for Daily Use. One of the common symptoms of COVID-19 that can be easily and noninvasively identified is high fever. Since the outbreak, a thermal screening strategy via infrared thermometers has been utilized in public areas to monitor individuals' body temperatures and subsequently identify potentially infected people in the community. This prevention is still lacking because it takes notable time to check the body temperature of every person at a large area. The crucial point is that the close contact of the infected person might spread the disease to the noninfected person who is checking the temperature. To tackle these challenges, a study was introduced to detect infection automatically from thermal images, requiring fewer human interactions via a smart helmet called a "Mounted Thermal Imaging System". Thermal camera technology was integrated into this smart helmet along with IoT technology for real-time monitoring. In addition, this system was equipped with facial recognition technology that could display personal information

as well. This design has a high demand from the healthcare system and would potentially slow the spread of infection more effectively.¹⁷¹

Similar to the smart helmet, IoT-based smart glasses have been introduced. With these smart glasses, high body temperature can be detected in a crowded environment and the measured data can be transferred to a mobile phone application. Using Google location history to provide reliable data about the detection process, the information about the locations where the suspected individuals are located can be included to the mobile platforms. This preliminary study and the proposed design would make a remarkable contribution to reduce scan time, especially by minimizing the possibility of virus spread.¹⁷²

Besides, a set of data algorithms have been designed to capture the early onsets and symptoms associated with COVID-19 infection through a wearable device in order to track patients easily as the disease progresses.¹⁷³ Briefly, an all-day wearable device generates continuous data streams and employs AI to potentially bring out life-saving insights. A soft, flexible, and cordless device with a size of a postage stamp is placed right below a thin suprasternal notch. Herein, the device monitors multiple parameters like cough intensity and types, chest wall movements, breathing sounds, heart rate, and body temperature. The collected data is transmitted automatically to a cloud system, where automated algorithms produce graphical summaries adapted to facilitate remote monitoring, even at home. Most importantly, real-time data flow from patients provides crucial and timely information about the symptoms and their consequences that are not detected by traditional monitoring systems. With an algorithm becoming smarter in the following stages, it is projected that coughs will be differentiated from another COVID-19-like and benign disease. Early detection of the disease would offer important and unique features to control the pandemic with these real-time, noninvasive, and smart devices.

Talking over the integration of biosensing strategies with mobile phone platforms, a colorimetric RT-LAMP assay was reported in detecting SARS-CoV-2 from clinical samples.¹⁷⁴ This system does not require any RNA isolation, so samples with swabs can be directly used. The color change of samples (red to yellow) could be determined within 30 min after the incubation process, and this change is simply determined by the camera of a regular mobile phone with basic features. In another paper-based LAMP assay that can be integrated with a smartphone application, people who are quarantined at home will be able to easily collect their nasal swabs and perform this test.¹⁷⁵ After observing colorimetric test results, they can record and share them with healthcare professionals using an application on their phone.

In addition, presymptomatic individuals cannot be identified with current test methods, hindering early diagnosis and the required intervention. Based on this shortcoming, the use of wearable devices for an early diagnosis of COVID-19 and screening physiological parameters for real-time health monitoring and surveillance has been investigated.¹⁷⁶ The study showed that heart rate signals obtained from smart watches can be used to detect COVID-19 infection long before symptom onset. Using the data obtained, they observed that high resting heart rates and outlying heart rate/step measurements generally changed before symptoms appeared, hence accelerating the early detection of COVID-19 infection at or before symptom onset.

CONCLUSION

Today, the world faces an immense viral respiratory disease outbreak, i.e., COVID-19, affecting over ~250 million people worldwide, and more than 5 million individuals have died over two years. In addition to leading to an unexpected public health crisis globally,¹⁷⁷ COVID-19 has had severe consequences across the globe, including physiologic, socio-economic, and political burdens that not only impose severe distress for patients and caregivers but also lead to enormous economic burden of up to \$82.4 trillion over five years,¹⁷⁸ as well as leading to governmental decisions to manage the “new normal”. Considering the other recent outbreaks, the total COVID-19 cases have already outnumbered the total cases of SARS and MERS together.¹⁷⁹ Consequently, COVID-19 is the most astounding healthcare challenge that people have faced in the 21st century.³⁶

The lessons taken from the pandemic explicitly state that early diagnosis is the mainstay to initiate the most efficient therapy, greatly accelerating life-saving decisions on treatment, contributing to the control and potential prevention of an emerging pandemic. Hence, WHO has been urging all communities to perform massive diagnostic testing to curb virus transmission, since testing aids researchers in learning the disease epidemiology. Despite centralized, well-equipped diagnostic facilities in developed countries, accessing diagnostic testing in the resource-scare settings is still a huge concern due to economic and technological shortfalls in the healthcare system.⁴⁵

From the detection perspective, conventional procedures mainly detect either SARS-CoV-2 target viral genome (direct detection) or immunoglobins (Ig) produced against virus immunogenic S proteins (indirect detection-serological assays). Because viral genetic code was released, COVID-19 diagnosis can be conventionally carried out by the means of PCR strategies as the gold standard method. However, many impediments limit its expansion to the POC settings³⁶ that include lengthy assay time with labor-intensive steps, and the requirement for highly trained personnel, specialized handling, and precise transportation conditions due to possible denaturation of genetic material. LFAs are mainly projected to detect serological information against the infection, providing an easy-to-use fashion to accelerate its expansion to home settings. Yet, this strategy is restricted with antibody levels and the lag phase for the level of antibody production to reach the LOD of the assay.³⁶ Besides, imaging techniques are widely utilized in the diagnosis of respiratory infections, but they are restricted to specialized healthcare centers and cannot be deployed to the POC and the resource-scare settings. Consequently, all these impediments guide us to develop alternative platforms to ease the way people are diagnosed currently.

Moving forward, biosensing holds one of the most promising strategies to curb the pandemic and to democratize all of these opportunities through versatile modalities that demonstrate unprecedented integration of sensors, bioanalytical methods, connectivity, and computing. Highlighting some of them, the list would include but not be limited to (i) the special unity of well-known electrochemical strategies with smart materials such as graphene FET;¹⁰⁶ (ii) the metamorphosis of molecular biology technologies such as CRISPR and their integration with easy-to-use LFAs in detecting viruses with low LODs and short-assay time;^{180,181} (iii) the hybridization of amplification-

free CRISPR methods and optical biosensors that monitor plasmonic photothermal effect and localized SP resonances;¹ (iv) a naked-eye detection of viral nucleic acids through plasmonic nanoparticles;¹⁸² (v) the monitoring strategies combining drones with IoT-based platforms to ensure the implementation of quarantine and mask-wearing;¹⁶⁶ (vi) the reduction of workload at hospitals through analyzing CT results via AI-stemmed approaches;¹⁶⁸ and (vii) the monitoring of certain symptoms, such as cough and body temperatures via band-aid and helmet type wearable devices.^{171,173}

Overall, the COVID-19 pandemic has provided us a crucial reminder to prepare ourselves in advance for such outbreaks to dampen their effects on the community. All the efforts in many research directions, especially in the biosensing realm, have exhibited a clear picture to handle the current status with minimal damage. As elaborated, detecting the disease at early stages via molecular biomarkers or any physiological symptoms would ease the clinical management of this malady. Adapting these technologies into daily life would enable easy and real-time monitoring to control clinical administration, as well as helping to manage the spread of the disease. In the first quarter of the 21st century, we have faced the significance of science and technology in tackling real-world challenges in medicine, and today we need science and technology more than we ever did before.

AUTHOR INFORMATION

Corresponding Author

Fatih Inci – UNAM–National Nanotechnology Research Center and Institute of Materials Science and Nanotechnology, Bilkent University, 06800 Ankara, Turkey; orcid.org/0000-0002-9918-5038; Email: finci@bilkent.edu.tr

Authors

Özgecan Erdem – UNAM–National Nanotechnology Research Center, Bilkent University, 06800 Ankara, Turkey
Ismail Eş – UNAM–National Nanotechnology Research Center, Bilkent University, 06800 Ankara, Turkey
Yeşeren Saylan – Department of Chemistry, Hacettepe University, 06800 Ankara, Turkey

Complete contact information is available at:

<https://pubs.acs.org/10.1021/acs.analchem.1c04454>

Notes

The authors declare no competing financial interest.

Biographies

Özgecan Erdem is a researcher at Bilkent University–UNAM. In 2014, she completed her Master's degree, where she performed research on fungal-assisted bioremediation of textile effluents. During her Ph.D. studies, she designed and synthesized imprinted polymers at molecular scale, which were then integrated with optical sensors to detect microorganisms from real-world samples. In addition, she was selected as a Sancar Fellow through the consortium between Hacettepe University and Bilkent University–UNAM in 2020. At the Incilab, she has been working on the development of point-of-care devices for the diagnosis of microorganisms, holding devastating impact on public health.

Ismail Eş graduated from the Department of Bioengineering at Ege University. He received his Master's degree in Genetics and Molecular Biology from the Federal University of Goiás (Brazil). He concluded his Ph.D. in the School of Chemical Engineering at the University of

Campinas (Brazil). During his Ph.D. studies, he manufactured microfluidic technology to synthesize lipid-based gene delivery systems. Between 2019 and 2021, he worked at University College London. His research at UCL focused on the fabrication of tumor-on-a-chip models and microfluidic systems to increase the productivity of viral particles. Recently, Dr. Eş has joined the Incilab and he currently works with the fabrication of metamaterial sensor production and biomarker detection.

Yeşeren Saylan is currently working as an assistant professor at Hacettepe University, Ankara, Turkey. She graduated from Hacettepe University, Department of Chemistry, in 2008. She then received her M.Sc. and Ph.D. degrees from Hacettepe University, Department of Chemistry, Division of Biochemistry, in 2011 and 2017, respectively. She worked as a visiting researcher at Stanford University, School of Medicine, and Harvard Medical School–Brigham and Women's Hospital. She is particularly dedicated to developing precise sensing platforms for medical diagnostics, environmental monitoring, and food safety, as well as rationally designing specific molecularly imprinted polymeric materials at micro and nanoscales for various applications.

Fatih Inci is an assistant professor at Bilkent University–UNAM. Earlier, he worked as an academician and postdoctoral researcher at Stanford University School of Medicine, Harvard Medical School–Brigham and Women's Hospital, and Harvard–MIT. His research focuses on the development of microfluidics and biosensors for medical diagnostics. He has published 50+ papers, 8 book chapters (3 chapters in-progress), and 3 editorials; edited 3 books (2 books in-progress). He holds 8 patents (issued/submitted) and 2 licensed products, and his work has been highlighted by NIH–NIBIB, NIJ, Science–AAAS, Nature Medicine, AIP, JAMA, Newsweek, and Popular Science.

ACKNOWLEDGMENTS

F.I. gratefully acknowledges the support of TÜBİTAK 2232–International Fellowship for Outstanding Researchers (project no: 118C254). This publication has been produced benefiting from the 2232 International Fellowship for Outstanding Researchers Program of TÜBİTAK (project no: 118C254). However, the entire responsibility for the article belongs to the owner of the article. The financial support received from TÜBİTAK does not mean that the content of the publication is approved in a scientific sense by TÜBİTAK. F.I. and Y.S. greatly acknowledge the financial support of TÜBİTAK 1001–The Scientific and Technological Research Projects Funding Program (project no: 120Z445). F.I. and I.E. are thankful for the financial support of TÜBİTAK 3501–Career Development Program (CAREER) (project no: 120Z335). Ö.E. gratefully acknowledges the support of the SANCAR Fellowship from Hacettepe–Bilkent University–UNAM. This work was supported by the BAGEP Award of the Science Academy.

REFERENCES

- (1) Qiu, G.; Gai, Z.; Tao, Y.; Schmitt, J.; Kullak-Ublick, G. A.; Wang, J. *ACS Nano* **2020**, *14* (5), 5268–5277.
- (2) Smith, R. D. *Soc. Sci. Med.* **2006**, *63* (12), 3113–3123.
- (3) Ding, Y.; He, L.; Zhang, Q.; Huang, Z.; Che, X.; Hou, J.; Wang, H.; Shen, H.; Qiu, L.; Li, Z.; Geng, J.; Cai, J.; Han, H.; Li, X.; Kang, W.; Weng, D.; Liang, P.; Jiang, S. *J. Pathol.* **2004**, *203* (2), 622–630.
- (4) Chinese SARS Molecular Epidemiology Consortium. *Science (Washington, DC, U. S.)* **2004**, *303* (5664), 1666–1669.
- (5) World Health Organization. Summary of probable SARS cases with onset of illness from 1 November 2002 to 31 July 2003. <https://>

www.who.int/publications/m/item/summary-of-probable-sars-cases-with-onset-of-illness-from-1-november-2002-to-31-july-2003.

- (6) Holmes, K. V. *J. Clin. Invest.* **2003**, *111* (11), 1605–1609.
- (7) Hilgenfeld, R.; Peiris, M. *Antiviral Res.* **2013**, *100* (1), 286–295.
- (8) de Wit, E.; van Doremalen, N.; Falzarano, D.; Munster, V. J. *Nat. Rev. Microbiol.* **2016**, *14* (8), 523–534.
- (9) Al-Tawfiq, J. A.; Memish, Z. A. *Microbiol. Respir. Syst. Infect.* **2016**, *55*–63.
- (10) Reusken, C. B. E. M.; Haagmans, B. L.; Müller, M. A.; Gutierrez, C.; Godeke, G.-J.; Meyer, B.; Muth, D.; Raj, V. S.; Smits-De Vries, L.; Corman, V. M.; et al. *Lancet Infect. Dis.* **2013**, *13* (10), 859–866.
- (11) Haagmans, B. L.; Al Dhahiry, S. H. S.; Reusken, C. B. E. M.; Raj, V. S.; Galiano, M.; Myers, R.; Godeke, G.-J.; Jonges, M.; Farag, E.; Diab, A.; et al. *Lancet Infect. Dis.* **2014**, *14* (2), 140–145.
- (12) Rothan, H. A.; Byrareddy, S. N. *J. Autoimmun.* **2020**, *109*, 102433.
- (13) Zhu, N.; Zhang, D.; Wang, W.; Li, X.; Yang, B.; Song, J.; Zhao, X.; Huang, B.; Shi, W.; Lu, R.; Niu, P.; Zhan, F.; Ma, X.; Wang, D.; Xu, W.; Wu, G.; Gao, G. F.; Tan, W. N. *Engl. J. Med.* **2020**, *382* (8), 727–733.
- (14) Lai, C. C.; Shih, T. P.; Ko, W. C.; Tang, H. J.; Hsueh, P. R. *Int. J. Antimicrob. Agents* **2020**, *55* (3), 105924.
- (15) Fanelli, D.; Piazza, F. *Chaos, Solitons Fractals* **2020**, *134*, 109761.
- (16) Luan, J.; Lu, Y.; Jin, X.; Zhang, L. *Biochem. Biophys. Res. Commun.* **2020**, *526* (1), 165–169.
- (17) Hoffmann, M.; Kleine-Weber, H.; Schroeder, S.; Krüger, N.; Herrler, T.; Erichsen, S.; Schiergens, T. S.; Herrler, G.; Wu, N. H.; Nitsche, A.; Müller, M. A.; Drosten, C.; Pöhlmann, S. *Cell* **2020**, *181*, 271.
- (18) Andersen, K. G.; Rambaut, A.; Lipkin, W. I.; Holmes, E. C.; Garry, R. F. *Nat. Med.* **2020**, *26*, 450.
- (19) Wang, Q.; Zhang, Y.; Wu, L.; Niu, S.; Song, C.; Zhang, Z.; Lu, G.; Qiao, C.; Hu, Y.; Yuen, K.-Y.; Wang, Q.; Zhou, H.; Yan, J.; Qi, J. *Cell* **2020**, *181*, 894.
- (20) Qiu, Y.; Zhao, Y.-B.; Wang, Q.; Li, J.-Y.; Zhou, Z.-J.; Liao, C.-H.; Ge, X.-Y. *Microbes Infect.* **2020**, *22* (4), 221–225.
- (21) Letko, M.; Marzi, A.; Munster, V. *Nat. Microbiol.* **2020**, *5* (4), 562–569.
- (22) Wang, Y.; Grunewald, M.; Perlman, S.; Maier, H. J.; Bickerton, E. *Methods Mol. Biol.* **2020**, *2203*, 1–29.
- (23) De Maio, F.; Lo Cascio, E.; Babini, G.; Sali, M.; Della Longa, S.; Tilocca, B.; Roncada, P.; Arcovito, A.; Sanguinetti, M.; Scambia, G.; Urbani, A. *Microbes Infect.* **2020**, *22* (10), 592–597.
- (24) Mousavizadeh, L.; Ghasemi, S. *J. Microbiol. Immunol. Infect.* **2021**, *54* (2), 159–163.
- (25) Wong, N. A.; Saier, M. H. *Int. J. Mol. Sci.* **2021**, *22* (3), 1308.
- (26) Ye, Q.; West, A. M. V.; Silletti, S.; Corbett, K. D. *Protein Sci.* **2020**, *29* (9), 1890–1901.
- (27) CDC. *Interim Guidelines for Clinical Specimens for COVID-19*. <https://www.cdc.gov/coronavirus/2019-ncov/lab/guidelines-clinical-specimens.html>.
- (28) Poon, L. L. M.; Chan, K. H.; Wong, O. K.; Yam, W. C.; Yuen, K. Y.; Guan, Y.; Lo, Y. M. D.; Peiris, J. S. M. *J. Clin. Virol.* **2003**, *28* (3), 233–238.
- (29) Noh, J. Y.; Yoon, S. W.; Kim, D. J.; Lee, M. S.; Kim, J. H.; Na, W.; Song, D.; Jeong, D. G.; Kim, H. K. *Arch. Virol.* **2017**, *162* (6), 1617–1623.
- (30) Meyer, B.; Drosten, C.; Müller, M. A. *Virus Res.* **2014**, *194*, 175–183.
- (31) Lamers, M. M.; Beumer, J.; van der Vaart, J.; Knoops, K.; Puschhof, J.; Breugem, T. I.; Ravelli, R. B. G.; Paul van Schayck, J.; Mykytyn, A. Z.; Duimel, H. Q.; van Donselaar, E.; Riesebosch, S.; Kuijpers, H. J. H.; Schipper, D.; van de Wetering, W. J.; de Graaf, M.; Koopmans, M.; Cuppen, E.; Peters, P. J.; Haagmans, B. L.; Clevers, H. *Science (Washington, DC, U. S.)* **2020**, *369* (6499), 50–54.
- (32) Tang, Y.-W. W.; Schmitz, J. E.; Persing, D. H.; Stratton, C. W. *J. Clin. Microbiol.* **2020**, *58* (6), e00512–20.
- (33) Bryan, A.; Pepper, G.; Wener, M. H.; Fink, S. L.; Morishima, C.; Chaudhary, A.; Jerome, K. R.; Mathias, P. C.; Greninger, A. L. *J. Clin. Microbiol.* **2020**, *58*, 15–16.
- (34) Long, Q.-X.; Liu, B.-Z.; Deng, H.-J.; Wu, G.-C.; Deng, K.; Chen, Y.-K.; Liao, P.; Qiu, J.; Lin, Y.; Cai, X.-F.; Wang, D.; Hu, Y.; Ren, J.; Tang, N.; Xu, Y.; Yu, L.; Mo, Z.; Gong, F.; Zhang, X. X.; Tian, W.; Hu, L.; Zhang, X. X.; Xiang, J.; Du, H.; Liu, H.; Lang, C.; Luo, X.; Wu, S.; Cui, X.; Zhou, Z.; Zhu, M.; Wang, J.; Xue, C.; Li, X.; Wang, L.; Li, Z.; Wang, K.; Niu, C.; et al. *Nat. Med.* **2020**, *26*, 845.
- (35) Udugama, B.; Kadhiresan, P.; Kozlowski, H. N.; Malekjahani, A.; Osborne, M.; Li, V. Y. C. C.; Chen, H.; Mubareka, S.; Gubbay, J. B.; Chan, W. C. W. *ACS Nano* **2020**, *14* (4), 3822–3835.
- (36) Morales-Narváez, E.; Dincer, C. *Biosens. Bioelectron.* **2020**, *163*, 112274.
- (37) Douglas, C. E.; Kulesh, D. A.; Jaissle, J. G.; Minogue, T. D. *Mol. Cell. Probes* **2015**, *29* (6), 511–513.
- (38) Hu, B.; Zeng, L.-P.; Yang, X.-L.; Ge, X.-Y.; Zhang, W.; Li, B.; Xie, J.-Z.; Shen, X.-R.; Zhang, Y.-Z.; Wang, N.; Luo, D.-S.; Zheng, X.-S.; Wang, M.-N.; Daszak, P.; Wang, L.-F.; Cui, J.; Shi, Z.-L. *PLoS Pathog.* **2017**, *13* (11), e1006698–e1006698.
- (39) Wang, P.; Anderson, N.; Pan, Y.; Poon, L.; Charlton, C.; Zelyas, N.; Persing, D.; Rhoads, D.; Babcock, H. *Clin. Chem.* **2020**, *66* (5), 644–651.
- (40) Chan, J. F.-W.; Yip, C. C.-Y.; To, K. K.-W.; Tang, T. H.-C.; Wong, S. C.-Y.; Leung, K.-H.; Fung, A. Y.-F.; Ng, A. C.-K.; Zou, Z.; Tsoi, H.-W.; Choi, G. K.-Y.; Tam, A. R.; Cheng, V. C.-C.; Chan, K.-H.; Tsang, O. T.-Y.; Yuen, K.-Y. *J. Clin. Microbiol.* **2020**, *58* (5), e00310–20.
- (41) Liu, R.; Han, H.; Liu, F.; Lv, Z.; Wu, K.; Liu, Y.; Feng, Y.; Zhu, C. *Clin. Chim. Acta* **2020**, *505*, 172–175.
- (42) Wang, Y.; Kang, H.; Liu, X.; Tong, Z. *J. Med. Virol.* **2020**, *92* (6), 538–539.
- (43) Infantino, M.; Damiani, A.; Gobbi, F. L.; Grossi, V.; Lari, B.; Macchia, D.; Casprini, P.; Veneziani, F.; Villalta, D.; Bizzaro, N.; Cappelletti, P.; Fabris, M.; Quartuccio, L.; Benucci, M.; Manfredi, M. *Isr. Med. Assoc. J.* **2020**, *22* (4), 203–210.
- (44) Yu, F.; Yan, L.; Wang, N.; Yang, S.; Wang, L.; Tang, Y.; Gao, G.; Wang, S.; Ma, C.; Xie, R.; Wang, F.; Tan, C.; Zhu, L.; Guo, Y.; Zhang, F. *Clin. Infect. Dis.* **2020**, *71* (15), 793–798.
- (45) Soler, M.; Estévez, M. C.; Cardenosa-Rubio, M.; Astua, A.; Lechuga, L. M. *ACS sensors* **2020**, *5* (9), 2663–2678.
- (46) Kosack, C. S.; Page, A. L.; Klatser, P. R. *Bull. World Health Organ.* **2017**, *95* (9), 639–645.
- (47) Wallis, L.; Blessing, P.; Dalwai, M.; Shin, S. Do *Glob. Health Action* **2017**, *10* (sup3), 1327686.
- (48) Zarei, M. *TrAC, Trends Anal. Chem.* **2017**, *91*, 26–41.
- (49) Yucel, M.; Akin, O.; Cayoren, M.; Akduman, I.; Palaniappan, A.; Liedberg, B.; Hizal, G.; Inci, F.; Yildiz, U. H. *Anal. Chem.* **2018**, *90* (8), 5122–5129.
- (50) Maduraveeran, G.; Sasidharan, M.; Ganesan, V. *Biosens. Bioelectron.* **2018**, *103*, 113–129.
- (51) Pandey, A.; Gurbuz, Y.; Ovguz, V.; Niazi, J. H.; Qureshi, A. *Biosens. Bioelectron.* **2017**, *91*, 225–231.
- (52) Schürmann, S.; Wagner, S.; Herlitze, S.; Fischer, C.; Gumbrecht, S.; Wirth-Hücking, A.; Pröhl, G.; Lautscham, L. A.; Faby, B.; Goldmann, W. H.; Nikolova-Krstevski, V.; Martinac, B.; Friedrich, O. *Biosens. Bioelectron.* **2016**, *81*, 363–372.
- (53) Inci, F.; Filippini, C.; Baday, M.; Ozen, M. O.; Calamak, S.; Durmus, N. G.; Wang, S.; Hanhauser, E.; Hobbs, K. S.; Juillard, F.; et al. *Proc. Natl. Acad. Sci. U. S. A.* **2015**, *112* (32), E4354–E4363.
- (54) Sender, R.; Bar-On, Y. M.; Gleizer, S.; Bernshtein, B.; Flamholz, A.; Phillips, R.; Milo, R. *Proc. Natl. Acad. Sci. U.S.A.* **2021**, *118* (25), e2024815118.
- (55) Khan, M. Z. H.; Hasan, M. R.; Hossain, S. I.; Ahommed, M. S.; Daizy, M. *Biosens. Bioelectron.* **2020**, *166*, 112431.
- (56) Fabiani, L.; Saroglia, M.; Galatà, G.; De Santis, R.; Fillo, S.; Luca, V.; Faggioni, G.; D’Amore, N.; Regalbutto, E.; Salvatori, P.; Terova, G.; Moscone, D.; Lista, F.; Arduini, F. *Biosens. Bioelectron.* **2021**, *171*, 112686.

- (57) Liv, L. *Microchem. J.* **2021**, *168*, 106445.
- (58) Mahari, S.; Roberts, A.; Shahdeo, D.; Gandhi, S. ECovSens-Ultrasonic Novel In-House Built Printed Circuit Board Based Electrochemical Device for Rapid Detection of NCovid-19 Antigen, a Spike Protein Domain 1 of SARS-CoV-2. *bioRxiv*, 2020. DOI: 10.1101/2020.04.24.059204
- (59) El-Said, W. A.; Al-Bogami, A. S.; Alshitari, W.; El-Hady, D. A.; Saleh, T. S.; El-Mokhtar, M. A.; Choi, J.-W. *BioChip J.* **2021**, *15* (3), 287–295.
- (60) Kim, H. E.; Schuck, A.; Lee, S. H.; Lee, Y.; Kang, M.; Kim, Y.-S. *Biosens. Bioelectron.* **2021**, *182*, 113168.
- (61) Liu, H.; Yang, A.; Song, J.; Wang, N.; Lam, P.; Li, Y.; Law, H. K.; Yan, F. *Sci. Adv.* **2021**, *7* (38), eabg8387.
- (62) Guo, K.; Wustoni, S.; Koklu, A.; Díaz-Galicia, E.; Moser, M.; Hama, A.; Alqahtani, A. A.; Ahmad, A. N.; Alhamlan, F. S.; Shuaib, M.; Pain, A.; McCulloch, I.; Arold, S. T.; Grünberg, R.; Inal, S. *Nat. Biomed. Eng.* **2021**, *5* (7), 666–677.
- (63) Song, Z.; Ma, Y.; Chen, M.; Ambrosi, A.; Ding, C.; Luo, X. *Anal. Chem.* **2021**, *93* (14), 5963–5971.
- (64) Li, Q.; Lu, N.; Wang, L.; Fan, C. *Small Methods* **2018**, *2* (4), 1700263.
- (65) Lee, R.; Kwon, D. W.; Kim, S.; Kim, S.; Mo, H.-S.; Kim, D. H.; Park, B.-G. *Jpn. J. Appl. Phys.* **2017**, *56* (12), 124001.
- (66) Malsagova, K. A.; Pleshakova, T. O.; Galiullin, R. A.; Kozlov, A. F.; Shumov, I. D.; Popov, V. P.; Tikhonenko, F. V.; Glukhov, A. V.; Ziborov, V. S.; Petrov, O. F.; et al. *Biosensors* **2020**, *10* (12), 210.
- (67) Gao, A.; Lu, N.; Dai, P.; Li, T.; Pei, H.; Gao, X.; Gong, Y.; Wang, Y.; Fan, C. *Nano Lett.* **2011**, *11* (9), 3974–3978.
- (68) Farzadfar, A.; Shayeh, J. S.; Habibi-Rezaei, M.; Omid, M. *Talanta* **2020**, *211*, 120722.
- (69) Tian, J.; Liang, Z.; Hu, O.; He, Q.; Sun, D.; Chen, Z. *Electrochim. Acta* **2021**, *387*, 138553.
- (70) Idili, A.; Parolo, C.; Alvarez-Diduk, R.; Merkoçi, A. *ACS Sensors* **2021**, *6* (8), 3093–3101.
- (71) Abrego-Martinez, J. C.; Jafari, M.; Chergui, S.; Pavel, C.; Che, D.; Sijaj, M. *Biosens. Bioelectron.* **2022**, *195*, 113595.
- (72) Ramanujam, A.; Almodovar, S.; Botte, G. G. *Processes* **2021**, *9* (7), 1236.
- (73) Tokel, O.; Inci, F.; Demirci, U. *Chem. Rev.* **2014**, *114* (11), 5728–5752.
- (74) Li, Z.; Leustean, L.; Inci, F.; Zheng, M.; Demirci, U.; Wang, S. *Biotechnol. Adv.* **2019**, *37* (8), 107440.
- (75) Inci, F.; Tokel, O.; Wang, S.; Gurkan, U. A.; Tasoglu, S.; Kuritzkes, D. R.; Demirci, U. *ACS Nano* **2013**, *7* (6), 4733–4745.
- (76) Ahmed, R.; Ozen, M. O.; Inci, F.; Karaaslan, M. G.; Henrich, T. J.; Demirci, U. *Proc.SPIE* **2019**, *10894*, 22.
- (77) Derin, E.; Erdem, Ö.; Inci, F. *Plasmonic Sensors and their Applications* **2021**, 1–22.
- (78) Inci, F.; Karaaslan, M. G.; Mataji-Kojouri, A.; Shah, P. A.; Saylan, Y.; Zeng, Y.; Avadhani, A.; Sinclair, R.; Lau, D. T.-Y.; Demirci, U. *Appl. Mater. Today* **2020**, *20*, 100709.
- (79) Mataji-Kojouri, A.; Ozen, M. O.; Shahabadi, M.; Inci, F.; Demirci, U. *ACS Nano* **2020**, *14* (7), 8518–8527.
- (80) Inci, F.; Celik, U.; Turken, B.; Özer, H. Ö.; Kok, F. N. *Biochem. Biophys. reports* **2015**, *2*, 115–122.
- (81) Ahmed, R.; Ozen, M. O.; Karaaslan, M. G.; Prator, C. A.; Thanh, C.; Kumar, S.; Torres, L.; Iyer, N.; Munter, S.; Southern, S.; Henrich, T. J.; Inci, F.; Demirci, U. *Adv. Mater.* **2020**, *32* (19), 1907160.
- (82) Inci, F.; Saylan, Y.; Kojouri, A. M.; Ogut, M. G.; Denizli, A.; Demirci, U. *Appl. Mater. Today* **2020**, *18*, 100478.
- (83) Djaileb, A.; Charron, B.; Jodaylami, M. H.; Thibault, V.; Coutu, J.; Forest, S.; Live, L. S.; Boudreau, D.; Pelletier, J. N.; Masson, J. A. Rapid and Quantitative Serum Test for SARS-CoV-2 Antibodies with Portable Surface Plasmon Resonance Sensing. *ChemRxiv*, 2020. DOI: 10.26434/chemrxiv.12118914.v1
- (84) Murillo, A. M. M.; Tomé-Amat, J.; Ramírez, Y.; Garrido-Arandia, M.; Valle, L. G.; Hernández-Ramírez, G.; Tramarin, L.; Herreros, P.; Santamaría, B.; Díaz-Perales, A.; Holgado, M. *Sens. Actuators, B* **2021**, *345*, 130394.
- (85) Huang, L.; Ding, L.; Zhou, J.; Chen, S.; Chen, F.; Zhao, C.; Xu, J.; Hu, W.; Ji, J.; Xu, H.; Liu, G. L. *Biosens. Bioelectron.* **2021**, *171*, 112685.
- (86) Lee, S.-L.; Kim, J.; Choi, S.; Han, J.; Seo, G.; Lee, Y. W. *Talanta* **2021**, *235*, 122801.
- (87) Chen, R.; Kan, L.; Duan, F.; He, L.; Wang, M.; Cui, J.; Zhang, Z.; Zhang, Z. *Microchim. Acta* **2021**, *188* (10), 316.
- (88) Jia, H.; Zhang, A.; Yang, Y.; Cui, Y.; Xu, J.; Jiang, H.; Tao, S.; Zhang, D.; Zeng, H.; Hou, Z.; Feng, J. *Lab Chip* **2021**, *21* (12), 2398–2406.
- (89) Liang, L. G.; Kong, M. Q.; Zhou, S.; Sheng, Y. F.; Wang, P.; Yu, T.; Inci, F.; Kuo, W. P.; Li, L. J.; Demirci, U.; Wang, S. Q. *Sci. Rep.* **2017**, *7* (March), 1–10.
- (90) Akceoglu, G. A.; Saylan, Y.; Inci, F. *Adv. Mater. Technol.* **2021**, *6*, 2100049.
- (91) Mani, V.; Paleja, B.; Larbi, K.; Kumar, P.; Tay, J. A.; Siew, J. Y.; Inci, F.; Wang, S.; Chee, C.; Wang, Y. T.; Demirci, U.; De Libero, G.; Singhal, A. *Sci. Rep.* **2016**, *6* (1), 35845.
- (92) Inan, H.; Wang, S.; Inci, F.; Baday, M.; Zangar, R.; Kesiraju, S.; Anderson, K. S.; Cunningham, B. T.; Demirci, U. *Sci. Rep.* **2017**, *7* (1), 3322.
- (93) Inci, F.; Karaaslan, M. G.; Gupta, R.; Avadhani, A.; Ogut, M. G.; Atila, E. E.; Duncan, G.; Klevan, L.; Demirci, U. *Forensic Sci. Int.: Genet.* **2021**, *52*, 102451.
- (94) Shirejini, S. Z.; Inci, F. *Biotechnol. Adv.* **2021**, 107814.
- (95) Deshmukh, S.; Inci, F.; Karaaslan, M. G.; Ogut, M. G.; Duncan, D.; Klevan, L.; Duncan, G.; Demirci, U. *Forensic Sci. Int.: Genet.* **2020**, *48*, 102313.
- (96) Nath, S.; Pigula, M.; Khan, A. P.; Hanna, W.; Ruhi, M. K.; Dehkordy, F. M.; Pushpavanam, K.; Rege, K.; Moore, K.; Tsujita, Y.; et al. *J. Clin. Med.* **2020**, *9* (4), 924.
- (97) Saylan, Y.; Erdem, Ö.; Inci, F.; Denizli, A. *Biomimetics* **2020**, *5* (2), 20.
- (98) Inci, F.; Ozen, M. O.; Saylan, Y.; Miansari, M.; Cimen, D.; Dhara, R.; Chinnasamy, T.; Yuksekkaya, M.; Filippini, C.; Kumar, D. K.; Calamak, S.; Yesil, Y.; Durmus, N. G.; Duncan, G.; Klevan, L.; Demirci, U. *Adv. Sci.* **2018**, *5* (9), 1800121.
- (99) Erdem, Ö.; Derin, E.; Sagdic, K.; Yilmaz, E. G.; Inci, F. *Emergent Mater.* **2021**, *4*, 169.
- (100) Xu, W.; Liu, J.; Song, D.; Li, C.; Zhu, A.; Long, F. *Microchim. Acta* **2021**, *188* (8), 261.
- (101) Zhao, B.; Che, C.; Wang, W.; Li, N.; Cunningham, B. T. *Talanta* **2021**, *225*, 122004.
- (102) Pietarinen, A.-V. *Methodology and Epistemology of Science: Metaphysics of Science*; 2011.
- (103) Afsahi, S.; Lerner, M. B.; Goldstein, J. M.; Lee, J.; Tang, X.; Bagarozzi, D. A.; Pan, D.; Locascio, L.; Walker, A.; Barron, F.; Goldsmith, B. R. *Biosens. Bioelectron.* **2018**, *100*, 85–88.
- (104) Terse-Thakoor, T.; Badhulika, S.; Mulchandani, A. J. *Mater. Res.* **2017**, *32* (15), 2905–2929.
- (105) Seo, G.; Lee, G.; Kim, M. J.; Baek, S.-H.; Choi, M.; Ku, K. B.; Lee, C.-S.; Jun, S.; Park, D.; Kim, H. G.; Kim, S.-J. S. II; Lee, J.-O.; Kim, B. T.; Park, E. C.; Kim, S.-J. S. II *ACS Nano* **2020**, *14* (4), 5135–5142.
- (106) Zhang, X.; Qi, Q.; Jing, Q.; Ao, S.; Zhang, Z.; Ding, M. Electrical Probing of COVID-19 Spike Protein Receptor Binding Domain via a Graphene Field-Effect Transistor. *arXiv* 2020. <https://arxiv.org/abs/2003.12529>.
- (107) Krsihna, B. V.; Ahmadsaidulu, S.; Teja, S. S. T.; Jayanthi, D.; Navaneetha, A.; Reddy, P. R.; Prakash, M. D. *Silicon* **2021**, DOI: 10.1007/s12633-021-01372-1.
- (108) Li, J.; Wu, D.; Yu, Y.; Li, T.; Li, K.; Xiao, M.-M.; Li, Y.; Zhang, Z.-Y.; Zhang, G.-J. *Biosens. Bioelectron.* **2021**, *183*, 113206.
- (109) Fathi-Hafshejani, P.; Azam, N.; Wang, L.; Kuroda, M. A.; Hamilton, M. C.; Hasim, S.; Mahjouri-Samani, M. *ACS Nano* **2021**, *15* (7), 11461–11469.
- (110) Kotov, N. A. *Nature* **2006**, *442* (7100), 254–255.

- (111) Shao, W.; Shurin, M. R.; Wheeler, S. E.; He, X.; Star, A. *ACS Appl. Mater. Interfaces* **2021**, *13* (8), 10321–10327.
- (112) Shrivastava, S.; Trung, T. Q.; Lee, N. E. *Chem. Soc. Rev.* **2020**, *49* (6), 1812–1866.
- (113) Koczula, K. M.; Gallotta, A. *Essays Biochem.* **2016**, *60* (1), 111–120.
- (114) Wen, T.; Huang, C.; Shi, F.-J.; Zeng, X.-Y.; Lu, T.; Ding, S.-N.; Jiao, Y.-J. *Analyst* **2020**, *145* (15), 5345–5352.
- (115) Chen, X.; Zhou, Q.; Li, S.; Yan, H.; Chang, B.; Wang, Y.; Dong, S. *Front. Cell. Infect. Microbiol.* **2021**, *11*, 656.
- (116) Roda, A.; Cavallera, S.; Di Nardo, F.; Calabria, D.; Rosati, S.; Simoni, P.; Colitti, B.; Baggiani, C.; Roda, M.; Anfossi, L. *Biosens. Bioelectron.* **2021**, *172*, 112765.
- (117) Pisanic, N.; Randad, P. R.; Kruczynski, K.; Manabe, Y. C.; Thomas, D. L.; Pekosz, A.; Klein, S. L.; Betenbaugh, M. J.; Clarke, W. A.; Laeyendecker, O.; Caturegli, P. P.; Larman, H. B.; Detrick, B.; Fairley, J. K.; Sherman, A. C.; Roupheal, N.; Edupuganti, S.; Granger, D. A.; Granger, S. W.; Collins, M. H.; Heaney, C. D.; Loeffelholz, M. J. *J. Clin. Microbiol.* **2020**, *59* (1), e02204–20.
- (118) Chen, P.-Y.; Ko, C.-H.; Wang, C. J.; Chen, C.-W.; Chiu, W.-H.; Hong, C.; Cheng, H.-M.; Wang, I.-J. *PLoS One* **2021**, *16* (7), e0254486.
- (119) Liu, D.; Shen, H.; Zhang, Y.; Shen, D.; Zhu, M.; Song, Y.; Zhu, Z.; Yang, C. *Lab Chip* **2021**, *21* (10), 2019–2026.
- (120) Baker, A. N.; Richards, S.-J.; Guy, C. S.; Congdon, T. R.; Hasan, M.; Zwetsloot, A. J.; Gallo, A.; Lewandowski, J. R.; Stansfeld, P. J.; Straube, A.; Walker, M.; Chessa, S.; Pergolizzi, G.; Dedola, S.; Field, R. A.; Gibson, M. I. *ACS Cent. Sci.* **2020**, *6* (11), 2046–2052.
- (121) Huang, C.; Wen, T.; Shi, F.-J.; Zeng, X.-Y.; Jiao, Y.-J. *ACS Omega* **2020**, *5* (21), 12550–12556.
- (122) Daoud, Z.; McLeod, J.; Stockman, D. L. *Front. Cell. Infect. Microbiol.* **2020**, *10*, 479.
- (123) Black, M. A.; Shen, G.; Feng, X.; Garcia Beltran, W. F.; Feng, Y.; Vasudevaraja, V.; Allison, D.; Lin, L. H.; Gindin, T.; Astudillo, M.; Yang, D.; Murali, M.; Iafate, A. J.; Jour, G.; Cotzia, P.; Snuderl, M. J. *Immunol. Methods* **2021**, *489*, 112909.
- (124) Li, Z.; Yi, Y.; Luo, X.; Xiong, N.; Liu, Y.; Li, S.; Sun, R.; Wang, Y.; Hu, B.; Chen, W.; Zhang, Y.; Wang, J.; Huang, B.; Lin, Y.; Yang, J.; Cai, W.; Wang, X.; Cheng, J.; Chen, Z.; Pan, K.; Pan, W.; Zhan, Z.; Chen, L.; Ye, F. *J. Med. Virol.* **2020**, *92* (9), 1518–1524.
- (125) Ragnosola, B.; Jin, D.; Lamb, C. C.; Shaz, B. H.; Hillyer, C. D.; Luchsinger, L. L. *BMC Res. Notes* **2020**, *13* (1), 372.
- (126) Chen, Z.; Zhang, Z.; Zhai, X.; Li, Y.; Lin, L.; Zhao, H.; Bian, L.; Li, P.; Yu, L.; Wu, Y.; Lin, G. *Anal. Chem.* **2020**, *92* (10), 7226–7231.
- (127) Zhou, Y.; Chen, Y.; Liu, W.; Fang, H.; Li, X.; Hou, L.; Liu, Y.; Lai, W.; Huang, X.; Xiong, Y. *Sens. Actuators, B* **2021**, *343*, 130139.
- (128) Wang, C.; Yang, X.; Gu, B.; Liu, H.; Zhou, Z.; Shi, L.; Cheng, X.; Wang, S. *Anal. Chem.* **2020**, *92* (23), 15542–15549.
- (129) Rideau, E.; Dimova, R.; Schwille, P.; Wurm, F. R.; Landfester, K. *Chem. Soc. Rev.* **2018**, *47* (23), 8572–8610.
- (130) Ghorbanizamani, F.; Tok, K.; Moulahoum, H.; Harmanci, D.; Hanoglu, S. B.; Durmus, C.; Zihnioglu, F.; Evran, S.; Cicek, C.; Sertoz, R.; Arda, B.; Goksel, T.; Turhan, K.; Timur, S. *ACS Sensors* **2021**, *6* (8), 2988–2997.
- (131) Zhu, X.; Wang, X.; Han, L.; Chen, T.; Wang, L.; Li, H.; Li, S.; He, L.; Fu, X.; Chen, S.; Xing, M.; Chen, H.; Wang, Y. *Biosens. Bioelectron.* **2020**, *166*, 112437.
- (132) Chen, R.; Ren, C.; Liu, M.; Ge, X.; Qu, M.; Zhou, X.; Liang, M.; Liu, Y.; Li, F. *ACS Nano* **2021**, *15* (5), 8996–9004.
- (133) Sibai, M.; Solis, D.; Röltgen, K.; Stevens, B. A.; Mfuh, K. O.; Sahoo, M. K.; Shi, R. Z.; Zehnder, J.; Boyd, S. D.; Pinsky, B. A. *J. Clin. Virol.* **2021**, *139*, 104818.
- (134) Liu, H.; Dai, E.; Xiao, R.; Zhou, Z.; Zhang, M.; Bai, Z.; Shao, Y.; Qi, K.; Tu, J.; Wang, C.; Wang, S. *Sens. Actuators, B* **2021**, *329*, 129196.
- (135) Aquino-Jarquín, G. *Nanomedicine* **2019**, *18*, 428–431.
- (136) Mustafa, M. I.; Makhawi, A. M. *J. Clin. Microbiol.* **2021**, *59* (3), e00745–20.
- (137) Chen, P.-Y.; Ko, C.-H.; Wang, C. J.; Chen, C.-W.; Chiu, W.-H.; Hong, C.; Cheng, H.-M.; Wang, I.-J. *PLoS One* **2021**, *16* (7), e0254486.
- (138) Bruch, R.; Baaske, J.; Chatelle, C.; Meirich, M.; Madlener, S.; Weber, W.; Dincer, C.; Urban, G. A. *Adv. Mater.* **2019**, *31* (51), 1905311.
- (139) Chen, P.-Y.; Ko, C.-H.; Wang, C. J.; Chen, C.-W.; Chiu, W.-H.; Hong, C.; Cheng, H.-M.; Wang, I.-J. *PLoS One* **2021**, *16* (7), e0254486.
- (140) Bhadra, S.; Riedel, T. E.; Lakhota, S.; Tran, N. D.; Ellington, A. D. *mSphere* **2021**, *6* (3), e00911–20.
- (141) Chekani-Azar, S.; Mombeni, E. G.; Birhan, M.; Yousefi, M. *J. Life Sci. Biomed* **2020**, *10* (1), 1–9.
- (142) Chekani-Azar, S.; Mombeni, E. G.; Birhan, M.; Yousefi, M. *J. Life Sci. Biomed* **2020**, *10* (1), 1–9.
- (143) Guo, L.; Sun, X.; Wang, X.; Liang, C.; Jiang, H.; Gao, Q.; Dai, M.; Qu, B.; Fang, S.; Mao, Y.; Chen, Y.; Feng, G.; Gu, Q.; Wang, R.; Zhou, Q.; Li, W. *Cell Discovery* **2020**, *6* (1), 1–4.
- (144) Broughton, J. P.; Deng, X.; Yu, G.; Fasching, C. L.; Servellita, V.; Singh, J.; Miao, X.; Streithorst, J. A.; Granados, A.; Sotomayor-gonzalez, A.; Zorn, K.; Gopez, A.; Hsu, E.; Gu, W.; Miller, S.; Pan, C.; Guevara, H.; Wadford, D. A.; Chen, J. S.; Chiu, C. Y. *Nat. Biotechnol.* **2020**, *38*, 870.
- (145) Broughton, J. P.; Deng, X.; Yu, G.; Fasching, C. L.; Servellita, V.; Singh, J.; Miao, X.; Streithorst, J. A.; Granados, A.; Sotomayor-gonzalez, A.; Zorn, K.; Gopez, A.; Hsu, E.; Gu, W.; Miller, S.; Pan, C.; Guevara, H.; Wadford, D. A.; Chen, J. S.; Chiu, C. Y. *Nat. Biotechnol.* **2020**, *38*, 870.
- (146) Li, S.; Huang, J.; Ren, L.; Jiang, W.; Wang, M.; Zhuang, L.; Zheng, Q.; Yang, R.; Zeng, Y.; Luu, L. D. W.; et al. *Talanta* **2021**, *233*, 122591.
- (147) Zhu, X.; Wang, X.; Li, S.; Luo, W.; Zhang, X.; Wang, C.; Chen, Q.; Yu, S.; Tai, J.; Wang, Y. *ACS sensors* **2021**, *6* (3), 881–888.
- (148) Broughton, J. P.; Deng, W.; Fasching, C. L.; Singh, J.; Chiu, C. Y.; Chen, J. S.; Charles, Y.; Chen, J. S.; Biosciences, M.; Francisco, S. S. S.; Francisco, S. S. S.; Francisco, S. S. S. *Mammoth Biosci. South San Fr. CA* **2020**, 1–9.
- (149) Zhou, C.; Su, F.; Pei, T.; Zhang, A.; Du, Y.; Luo, B.; Cao, Z.; Wang, J.; Yuan, W.; Zhu, Y.; Song, C.; Chen, J.; Xu, J.; Li, F.; Ma, T.; Jiang, L.; Yan, F.; Yi, J.; Hu, Y.; Liao, Y.; Xiao, H. *Geogr. Sustain.* **2020**, *1* (1), 77–87.
- (150) Cockcroft, J.; Avolio, A. *Curr. Hypertens. Rep.* **2020**, *22* (1), 9.
- (151) Alimadadi, A.; Aryal, S.; Manandhar, L.; Munroe, P. B.; Joe, B.; Cheng, X. *Physiol. Genomics* **2020**, *52* (4), 200–202.
- (152) Apple Newsroom. Apple and Google Partner on COVID-19 Contact Tracing Technology. 2020; p 1. <https://www.apple.com/newsroom/2020/04/apple-and-google-partner-on-covid-19-contact-tracing-technology/>.
- (153) Li, Y.; Liu, B.; Cui, J.; Wang, Z.; Shen, Y.; Xu, Y.; Yao, K.; Guan, Y. Similarities and Evolutionary Relationships of COVID-19 and Related Viruses. *Preprints* 2020, 2020030316. DOI: 10.20944/preprints202003.0316.v1.
- (154) Tilocca, B.; Soggiu, A.; Sanguinetti, M.; Musella, V.; Britti, D.; Bonizzi, L.; Urbani, A.; Roncada, P. *Microbes Infect.* **2020**, *22*, 188.
- (155) Uslupehlivan, M.; Şener, E. Glycoinformatics Approach for Identifying Target Positions to Inhibit Initial Binding of SARS-CoV-2 S1 Protein to the Host Cell. *bioRxiv*, 2020; 2020.03.25.
- (156) Wu, C.; Liu, Y.; Yang, Y.; Zhang, P.; Zhong, W.; Wang, Y.; Wang, Q.; Xu, Y.; Li, M.; Li, X.; Zheng, M.; Chen, L.; Li, H. *Acta Pharm. Sin. B* **2020**, *10* (5), 766–788.
- (157) Han, Y.; Král, P. *ACS Nano* **2020**, *14* (4), 5143–5147.
- (158) Shah, B.; Modi, P.; Sagar, S. R. *Life Sci.* **2020**, *252*, 117652.
- (159) Elmezayen, A. D.; Al-Obaidi, A.; Şahin, A. T.; Yelekcı, K. *J. Biomol. Struct. Dyn.* **2021**, *39*, 2980.
- (160) Zhu, H.; Podesva, P.; Liu, X.; Zhang, H.; Teply, T.; Xu, Y.; Chang, H.; Qian, A.; Lei, Y.; Li, Y.; Niculescu, A.; Iliescu, C.; Neuzil, P. *Sens. Actuators, B* **2020**, *303*, 127098.

- (161) Tuli, S.; Basumatary, N.; Gill, S. S.; Kahani, M.; Arya, R. C.; Wander, G. S.; Buyya, R. *Futur. Gener. Comput. Syst.* **2020**, *104*, 187–200.
- (162) Rahman, M. S.; Peeri, N. C.; Shrestha, N.; Zaki, R.; Haque, U.; Hamid, S. H. A. *Heal. policy Technol.* **2020**, *9* (2), 136–138.
- (163) Erdem, Ö.; Derin, E.; Zeibi Shirejini, S.; Sagdic, K.; Yilmaz, E. G.; Yildiz, S.; Akceoglu, G. A.; Inci, F. *Adv. Mater. Technol.* **2021**, 2100572.
- (164) Erdem, Ö.; Eş, I.; Akceoglu, G. A.; Saylan, Y.; Inci, F. *Biosensors* **2021**, *11* (9), 296.
- (165) Yang, T.; Gentile, M.; Shen, C. F.; Cheng, C. M. *Diagnostics* **2020**, *10* (4), 224.
- (166) Javaid, M.; Haleem, A.; Vaishya, R.; Bahl, S.; Suman, R.; Vaish, A. *Diabetes Metab. Syndr. Clin. Res. Rev.* **2020**, *14* (4), 419–422.
- (167) Madurai Elavarasan, R.; Pugazhendhi, R. *Sci. Total Environ.* **2020**, *725*, 138858.
- (168) Kummitha, R. K. R. *Gov. Inf. Q.* **2020**, *37*, 101481.
- (169) Wang, Z.; Tang, K. *Nat. Med.* **2020**, *26* (April), 458.
- (170) Jiang, X.; Coffee, M.; Bari, A.; Wang, J.; Jiang, X.; Huang, J.; Shi, J.; Dai, J.; Cai, J.; Zhang, T.; Wu, Z.; He, G.; Huang, Y. *Comput. Mater. Contin.* **2020**, *62* (3), 537–551.
- (171) Mohammed, M. N.; Syamsudin, H.; Al-Zubaidi, S.; A.K, S.; Ramli, R.; Yusuf, E.; AKS, R. R.; Yusuf, E. *Int. J. Psychosoc. Rehabil.* **2020**, *24* (7), 2296–2303.
- (172) Mohammed, M. N.; Hazairin, N. A.; Syamsudin, H.; Al-Zubaidi, S.; A.K, S.; Mustapha, S.; Yusuf, E. *Int. J. Adv. Sci. Technol.* **2020**, *29* (7), 954–960.
- (173) Morris, A. Monitoring COVID-19 from hospital to home: First wearable device continuously tracks key symptoms. *Norwestern Now* 2020. <https://news.northwestern.edu/stories/2020/04/monitoring-covid-19-from-hospital-to-home-first-wearable-device-continuously-tracks-key-symptoms/>.
- (174) Dao Thi, V. L.; Herbst, K.; Boerner, K.; Meurer, M.; Kremer, L. P.; Kirrmaier, D.; Freistaedter, A.; Papagiannidis, D.; Galmozzi, C.; Stanifer, M. L.; Boulant, S.; Klein, S.; Chlanda, P.; Khalid, D.; Barreto Miranda, I.; Schnitzler, P.; Krausslich, H.-G.; Knop, M.; Anders, S. *Sci. Transl. Med.* **2020**, *12* (556), eabc7075.
- (175) Yang, T.; Wang, Y.-C.; Shen, C.-F.; Cheng, C.-M. *Diagnostics* **2020**, *10* (3), 165.
- (176) Mishra, T.; Wang, M.; Metwally, A. A.; Bogu, G. K.; Brooks, A. W.; Bahmani, A.; Alavi, A.; Celli, A.; Higgs, E.; Dagan-Rosenfeld, O. Early Detection of Covid-19 Using a Smartwatch. *medRxiv*, 2020. DOI: 10.1101/2020.07.06.20147512
- (177) Fauci, A. S.; Lane, H. C.; Redfield, R. R. *N. Engl. J. Med.* **2020**, *382*, 1268–1269.
- (178) Centre for Risk Studies University of Cambridge Judge Business School. *The GDP@Risk over five years from COVID-19 could range from \$3.3 trillion to \$82 trillion, says the Centre for Risk Studies*; 2020. <https://www.jbs.cam.ac.uk/insight/2020/economic-impact/>.
- (179) Mahase, E. *BMJ.* **2020**, *368*, m641.
- (180) Sheridan, C. *Nat. Biotechnol.* **2020**, *38*, 515–518.
- (181) Zhang, F.; Abudayyeh, O. O.; Gootenberg, J. S. *A Protocol for Detection of COVID-19 Using CRISPR Diagnostics*; 2020; Vol. 8.
- (182) Moitra, P.; Alafeef, M.; Dighe, K.; Frieman, M. B.; Pan, D. *ACS Nano* **2020**, *14* (6), 7617–7627.
- (183) FIND (Foundation for Innovative New Diagnostics). SARS-CoV-2 diagnostic pipeline. <https://www.finddx.org/covid-19/pipeline/>.
- (184) Jiang, Y.; Hu, M.; Liu, A.-A.; Lin, Y.; Liu, L.; Yu, B.; Zhou, X.; Pang, D.-W. *ACS sensors* **2021**, *6* (3), 1086–1093.
- (185) Rossi, G. A.; Sacco, O.; Mancino, E.; Cristiani, L.; Midulla, F. *Infection* **2020**, *48* (5), 665–669.